Università degli Studi della Calabria

Dipartimento di Fisica

DOTTORATO DI RICERCA IN FISICA

XXII CICLO
FIS/03

TESI DI DOTTORATO

ENTANGLEMENT DYNAMICS IN A CAVITY AND ITS PROTECTION BY THE QUANTUM ZENO EFFECT

Supervisore
Dott. Francesco Plastina

Dottorando
Francesco Francica

Coordinatore
Prof. Giovanni Falcone

Anno Accademico 2008-2009

Table of Contents

Table of Contents

Chapter 1

Measures of bipartite entanglement

The aim of this first chapter is to review the meaning and definitions of some measures of entanglement, quantities able to quantify the entanglement encoded in a quantum state, that will be considered and employed in our research work reported in the following chapters.

The most important features of quantum entanglement, in particular, the non-local feature of strong correlation between the parts of a quantum system which is an intrinsically quantum effect and cannot be explained by classical theory [1, 2] are reviewed.

In sec. (1.1.1), we will see that the entanglement is well characterized and quantified if thought as a characteristic of the system which cannot be created by local operations (i.e., operations that act on parts separately distinguished), nor by operations coordinated through classical communications.

In sec.(1.2), we will illustrate an extension of the entropy of entanglement to mixed states, known as the entanglement of formation E_F. In general, in order to calculate the entanglement of formation one needs to perform a difficult minimization procedure. For qubits, this procedure can be carried out explicitly, and in sec.(1.3),

we discuss we show the result expressed in terms of the so-called concurrence, which , by itself, is a useful quantifier of entanglement for a two-qubit systems.

1.1 Measures of entanglement

The relevance of entanglement quantification stems from both a fundamental point of view and for potentially practical reasons. Indeed, we may treat entanglement as a resource, just as energy and information, needed to perform certain tasks, and therefore its measure becomes essential.

There are in principle two ways to quantify the entanglement in a state:

1. *Operational measures* are based on how well a certain task can be performed, usually compared to Bell states;

2. *Abstract measures* are based on the search of a set of natural axioms we believe an entanglement measure should satisfy.

The axiomatic approach in quantifying entanglement has been quite successful and measures have been defined that quantify certain aspects of entanglement. So far, there is no uniquely accepted list of axioms, however, the only absolute requirement has always been that entanglement, irrespective of how we quantify it, should not increase under *local operations and classical communication* (LOCC), i.e. it is monotonic under LOCC [3, 4, 5, 6].

In the following, we review this leading idea for quantifying entanglement, that is called *monotonicity condition.*

1.1.1 Entanglement monotones

The entanglement is a non-local quantum correlation between the parties of a composite system that doesn't have analogs in the classical physics [7].

Its importance not only resides in philosophical considerations about the nature of quantum theory, but also in the applications; in fact recently it has emerged that non-locality is the key resource both in quantum computation and communication, and it plays an important role in the cryptography

In effects, the presence of entanglement automatically provides an element of non-locality that often allows to overcome the classical limits of computation and communication.

In a bipartite system AB described by the space of Hilbert $\mathcal{H}_{AB}$, if the states ρ_A e ρ_B describes the single subsystems, then the most general separable state is given by the convex sum following

$$\rho = \sum_i p_i \rho_A^{(i)} \otimes \rho_B^{(i)} \tag{1.1}$$

where convexity implies positive coefficients p_i that sum up to unity, $\sum_i p_i = 1$. Such a state can contain *global classical correlations* (that is, it can have a non-local character), due to incomplete knowledge about the system state. These are characterized completely by the classical probabilities p_i. Then, the quantum correlations are certainly absent in such state, since it is only a statistic mixture of the states with weight p_i.

The typical example of entangled state is the spin singlet state, commonly known

as "EPR state", proposed by Bohm [8]

$$|\Psi\rangle_{AB} = \frac{1}{\sqrt{2}}\left(|01\rangle - |10\rangle\right) \tag{1.2}$$

In such case, as shown by Bell [2], the state shows *non-local quantum correlations*, stronger than those allowed by any local hidden variable model. Moreover the "GHZ state"

$$|\Psi\rangle_{ABC} = \frac{1}{\sqrt{2}}\left(|000\rangle + |111\rangle\right)$$

is a canonical example of state of a tripartite entangled system, for which non-local quantum correlations, that cannot classically be described, are shown in direct way, by a single realization and not only through statistic averages (as it happens for the singlet state).

These aspects of the quantum mechanics are reported as *quantum non-locality*, and they form an important part of the study of its foundations.

Both the classical and the quantum correlations can be non-local; nevertheless, they exhibit deeply different features. The *classical correlations* can easily to be produced by local operations coordinated through the exchange of classical information (LOOC).

Indeed, the local operations are the most general actions performed on a subsystem independently from the others; whereas the classical communications allow to correlate (classically) these local operations.

In a sentence, *the classical communication is admitted because it allows to create mixed states which are classically correlated but don't exhibit quantum correlations.*

On the other hand, the *entanglement* (non-local quantum correlations) is a non-local feature in a stronger sense: observers A and B having access to different parties of a bipartite system in a "locally well defined" state (product state) cannot create an entangled state with only LOOC operations.
Finally, in order to create entanglement an interaction between the parties of the composite system is needed.
If two subsystems are interacting with each other, their evolution will in general not derive from purely local operations. Any operation that is not local is called *global*. Under this type of operations all kinds of correlations can increase, as well as decrease. Therefore, entangled states can be created from initially separable states and vice-versa. The most prominent and natural way of creating entangled states is a global unitary evolution due to an interaction between subsystems.

Since a classical communication between the parties cannot increase the quantum correlation, we expect that any quantitative measure of entanglement should not be increase under LOOC. Further, such a measure must remain invariant under the action of all reversible LOCC protocols, one specific subclass of which is the set of local unitary transformations. This observation yields the intuitive result that the entanglement in a system is independent of the choice of local bases used to describe the subsystems. Finally, from the above discussion a result emerges that we can consider as: **Fundamental principle of the entanglement theory**

> *Entanglement cannot be created neither be increased under a set of local operations and classical communication (LOOC).*

The basic idea for a quantitative treatment is to classify all kinds of operations that

in principle can be applied to quantum systems and that can create or increase only classical correlations, but not that of quantum nature. Any quantity that is supposed to quantify entanglement needs to be monotonously decreasing under such operations[6, 3].

Any scalar valued function $\mathcal{M}(\rho)$ that satisfies this criterion is called an *entanglement monotone*.

Entanglement monotones that satisfy some additional axioms are called *entanglement measures* $E(\rho)$, scalar quantities that quantify quantum correlations, and distinguish them from classical ones. In the following we present a list of potential axioms that an entanglement measure should satisfy[6, 3]:

A1 $E(\rho) \geq 0$

A2 $E_X(\rho) = 0$ if ρ is separable

A3 (Normalisation): $E\Big(|\Psi^+\rangle\langle\Psi^+|\Big) = 1$ where $|\Psi^+\rangle = \frac{1}{\sqrt{2}}(|00\rangle + |11\rangle)$

M1 (LOCC monotonicity): for all density operators ρ and local operations $\Lambda_{i,k}$ performed by an observer k,

$$\mathcal{M}(\rho) \geq \sum_i p_i \mathcal{M}(\rho_i) \tag{1.3}$$

where

$$p_i = tr[\Lambda_{i,k}(\rho)] \qquad \rho_i = \frac{\Lambda_{i,k}(\rho)}{p_i}$$

M2 (Convexity - LOCC monotonicity under loss of information): for all ensemble decompositions $\{p_i, \rho_i\}$

$$\sum_i p_i \mathcal{M}(\rho_i) \geq \mathcal{M}(\rho) \tag{1.4}$$

where

$$\rho = \sum_i p_i \rho_i$$

Thus, entanglement monotones are specifically designed to detect and quantify only the quantum mechanical correlations in a composite system. In this context, the condition $M1$ from Eq(1.3) ensures monotonicity, on average, for any individual local operation, and hence for a general LOCC protocol. The second condition $M2$, Eq. (1.4), states that $\mathcal{M}(\rho)$ is a convex function which ensures that monotonicity is also preserved under mixing, i.e., when some of the information about the results of local operations is forgotten or is not communicated to the other party. Mixing of states does not increase entanglement.

For pure bipartite states it is rather simple to find some entanglement monotones due to the fact that there are no classical correlations contained in pure states. For mixed states the situation is much more involved, because there are both classical and quantum correlations that have to be discriminated against each other by an entanglement monotone. However, realistic states observed in experiments are mixed, since there is no system that could be decoupled perfectly from environmental influences, and mixing is thus unavoidable. Thus, an intensive research has been devoted to find a proper quantification also of mixed states entanglement.

Only for the simple case of two-qubit systems an explicit expression to quantify entanglement is obtainable, leading to the quantifier known as concurrence. This was originally introduced as an auxiliary quantity, used to calculate the entanglement of formation of two-qubit systems. However, concurrence can also be considered as an independent entanglement measure [9], which will be hereafter chosen for treating the entanglement dynamics.

1.2 Entanglement of formation

The entanglement of formation was historically the first entanglement measure to be proposed [3], and it results to be a straightforward generalization of the entropy of entanglement to mixed states.

Indeed, for a mixed state of a bipartite system, the von Neumann entropy of a subsystem is no longer a good measure of entanglement, because each subsystem can now have nonzero entropy on its own even if there is no entanglement in the original bipartite state. The entanglement of formation is designed to individuate the irreducible entanglement of the mixed state.

In general, as we will see, in order to calculate the entanglement of formation one needs to perform a difficult minimization procedure. Nevertheless, a connection to a related quantity particularly simple to evaluate, the concurrence, was established by Wootters [9]. Further, more important is that through this connection between the two measures of entanglement, the concurrence for mixtures, which arises as a purely mathematical generalization of that for pure states, can be interpreted operationally as a physically reasonable measure of entanglement for mixed states as well.

We imagine that the two observers Alice and Bob possessing the two parts of the bipartite system whose entanglement we are investigating, want to create n copies of a particular mixed state ρ to be shared between them. They initially share many singlet states [1] and are allowed no quantum communication.

[1] Initial entangled states are needed because the LOOC operations, that constitute the protocol of formation, cannot create entanglement.

Extending the results obtained in the case of pure state to an arbitrary bipartite mixed state ρ, with the pure state decomposition

$$\rho = \sum_i p_i |\Psi_i\rangle\langle\Psi_i| \tag{1.5}$$

one finds that the number of singlets needed to create this particular decomposition of ρ is given by

$$m = n \sum_i p_i E_S(\Psi_i)$$

that depends on the particular decomposition of ρ that was chosen.

Indeed, for each value of $i = 1, \ldots, N$, they create $n\,p_i$ copies of the pure state $|\Psi_i\rangle$ by using $n\,p_i\,E_S(\Psi_i)$ singlet pairs, where $E_S(\Psi_i)$ is the pure state entanglement. They will then have created a large ensemble of n pairs, discarding any possible record that would tell them which value of the index i to associate with each physical pair. At this point, then, each pair could be in any of the states $|\Psi_i\rangle$ with probability p_i; that is, each pair is now in the mixed state ρ.

Thus, for a given ensemble of pure states $\mathcal{E} = \{p_i, |\Psi_i\rangle\}$ the entanglement of formation could be defined as the average value of the entanglement of pure states of the ensemble

$$E_F(\mathcal{E}) \equiv \sum_i p_i E_S(\Psi_i) \tag{1.6}$$

However, a mixed state can be realized by many ensemble of pure states $\mathcal{E} = \{p_i, |\Psi_i\rangle\}$, with different entanglement of formation.

For instance, if ρ is the state of a two spin-$\frac{1}{2}$ particles

$$\rho = \frac{1}{2}\left(|00\rangle\langle 00| + |11\rangle\langle 11|\right)$$

it can be regarded either as an equal mixture of the pure states $|00\rangle$ and $|11\rangle$, or as an equal mixture of the pure Bell states $|\Phi^+\rangle = \frac{1}{\sqrt{2}}\left(|00\rangle + |11\rangle\right)$ and $|\Phi^-\rangle =$

$\frac{1}{\sqrt{2}}(|00\rangle - |11\rangle)$ [2]. To create an ensemble based on the former decomposition requires no singlets at all, since neither $|00\rangle$ nor $|11\rangle$ is entangled, while the second decomposition would require one singlet state for each copy of ρ.

In order to obtain a measure of the *minimum* number of singlet states utilized to create the state ρ, it is necessary to find the decomposition of ρ that minimizes the quantity of Eq(1.6).

These reasons motivate the definition of *entanglement of formation* of a mixed state [7, 3, 10] as the minimum value of the average entanglement of pure states of the ensemble if one considers all the possible ensemble decompositions of ρ, that is:

$$E_F(\rho) \equiv \inf_{\{p_i, |\Psi_i\rangle\}} \sum_i p_i E_S(|\Psi_i\rangle) \tag{1.7}$$

where the infimum is taken over all pure-state decompositions of ρ and $E_S(|\Psi_i\rangle)$ is the entanglement of the pure states.

Thus, the entanglement of formation has the physical meaning of quantification of the resources needed to create a given entangled state [3]. If one thus prepares the state ρ as a statistical mixture, then at least the entanglement of formation must be produced on the average.

The generalization of the entropy of entanglement, defined only for pure states, to the entanglement of formation, which is defined for both pure and mixed states, is a specific example of a convex-roof extension [11, 12, 13]. The method extends a measure valid on some sub-set (here, the pure states) to the convex hull[3] (here mixed states), where it is the largest function that is convex and compatible with the

[2] $\rho = \frac{1}{2}(|\Phi^+\rangle\langle\Phi^+| + |\Phi^-\rangle\langle\Phi^-|) = \frac{1}{2}(|00\rangle\langle 00| + |11\rangle\langle 11|)$

[3] The convex hull of a set is the set of all elements that can be written as a convex combination of the original set. For instance, the convex hull of two points is the line connecting them.

measure on the original set. More generally, any pure state entanglement monotone $E(\Psi)$ can be extended to mixed states by finding the minimum average value of the measure over all pure state ensemble decompositions of ρ [6]

$$E(\rho) \equiv \inf_{\{p_i, |\Psi_i\rangle\}} \sum_i p_i E(|\Psi_i\rangle) \tag{1.8}$$

where the resulting function $E(\rho)$ is the largest convex function of ρ that agrees with $E(\Psi)$ on all pure states. Vidal [6] demonstrated that any such function automatically satisfies conditions (1.3) and (1.4) of the entanglement monotone.

Unfortunately the above minimization procedure is notoriously difficult. Accordingly, closed forms for the entanglement of formation exist in only a very limited number of cases [9, 14, 15].

1.3 Concurrence

A concept related to the entanglement of formation is the *concurrence* [16, 9]. It is defined for a system of two qubits, and it has appeared useful to deduce analytical expressions that quantify entanglement in some classes of bipartite systems. We note that there exists no clear resource-based interpretation for the concurrence such as we have for the entanglement of formation. In this section we describe in detail such measure.

As a preparation for the generalization to mixed states, the definition of concurrence can be based on a specific transformation on the density operators, the *spin-flip* operation. To be more precise, we consider a pure state $|\Psi\rangle$. The spin-flip operation

applied to this state produces

$$|\widetilde{\Psi}\rangle = \sigma_y \otimes \sigma_y (|\Psi\rangle)^* \tag{1.9}$$

where σ_y is the usual Pauli operator which exchanges the states of the computational basis and inserts the relative phase $\pm i$, and * denotes complex conjugation, both taken in the computational basis. The operation in Eq (1.9) is clearly an antilinear operator[4].

For a pure state of two qubits, the concurrence is given by

$$\mathcal{C}(\Psi) \equiv \left| \langle \Psi | \widetilde{\Psi} \rangle \right| \tag{1.10}$$

The spin-flip operation maps the state of each qubit to its corresponding orthogonal state, i.e., the state diametrically opposite on the Bloch sphere. Thus, the concurrence of any product state is equal to zero as expected. Conversely, performing the spin-flip operation on a maximally entangled state, such as the singlet state $|\Psi^-\rangle$, leaves the state invariant (up to an overall phase), demonstrating that the concurrence achieves its maximum value, that results to be equal to one, for the maximally entangled states.

We also write the concurrence of a pure state as a function of the associated density operator $\rho = |\Psi\rangle\langle\Psi|$:

$$\begin{aligned} \mathcal{C}(\Psi)^2 &= \left| \langle \Psi | \widetilde{\Psi} \rangle \right|^2 = \langle \Psi | \widetilde{\Psi} \rangle \langle \widetilde{\Psi} | \Psi \rangle \\ &= \mathrm{tr} \left[\, |\Psi\rangle\langle\Psi| \widetilde{\Psi}\rangle\langle\widetilde{\Psi}| \, \right] \\ &= \mathrm{tr} \left[\, \rho \, \widetilde{\rho} \, \right] \end{aligned} \tag{1.11}$$

[4] An antilinear operator θ is an operator that satisfies the relationship $\theta(c_1|\phi_1\rangle + c_2|\phi_2\rangle) = c_1^* \theta|\phi_1\rangle + c_2^* \theta|\phi_2\rangle$.

where the operator $\rho\,\widetilde{\rho}$ is obtained from

$$\widetilde{\rho} \equiv (\,\sigma_y \otimes \sigma_y\,)\,\rho^*\,(\,\sigma_y \otimes \sigma_y\,)$$

and the tilde again denotes the spin-flip of the quantum state.

The importance of this representation is that it suggests an initially formal generalization of the concurrence to mixed states.

More generally, the following relationship holds between the concurrence and the entropy of entanglement [17], which for pure states represents the natural measure of entanglement,

$$E_S(\Psi) = \mathcal{E}(\mathcal{C}(\Psi))$$

where the function $\mathcal{E}$ is defined by

$$\mathcal{E}(\mathcal{C}) \equiv h\left(\frac{1+\sqrt{1-\mathcal{C}^2}}{2}\right) \tag{1.12}$$

and

$$h(x) \equiv -x\log_2 x - (1-x)\log_2(1-x)$$

is the binary entropy of the parameter x.

The connection between concurrence and entanglement is particularly clear if we express the state in the computational basis:

$$|\Psi\rangle = a|00\rangle + b|01\rangle + c|10\rangle + d|11\rangle$$

It is easy to verify that $|\Psi\rangle$ is separable if and only if $ad = bc$, so that we can take the difference between ad e bc as a measure of entanglement. Indeed, the concurrence turns out to be

$$\mathcal{C}(\Psi) = 2\,|ad - bc|$$

That the concurrence satisfies the requirements for being an entanglement monotone follows immediately from the observation that $\mathcal{E}(\mathcal{C})$ is a monotonically increasing function of C and vice-versa.

The concurrence is monotonic under LOCC, and can thus be used as an entanglement measure for two qubits. The great advantage is that it is easily computable. But more important is that it is directly related to the entanglement of formation, providing an explicit formula for the entanglement of formation in the case of two qubits.

The generalization of the concurrence to a mixed state of two qubits proceeds by taking the convex-roof extension according to Eq(1.8). In this way, for a mixed state $\rho = \sum_i p_i |\Psi_i\rangle\langle\Psi_i|$ follows

$$\mathcal{C}(\rho) \equiv \inf_{\{p_i, |\Psi_i\rangle\}} \sum_i p_i \mathcal{C}(\Psi_i) = \inf_{\{p_i, |\Psi_i\rangle\}} \sum_i p_i \left| \langle \Psi_i | \widetilde{\Psi}_i \rangle \right| \tag{1.13}$$

that is the average concurrence of the pure states of the decomposition, minimized over all the possible decompositions of ρ.

We observe that the function $\mathcal{E}(\mathcal{C})$ of Eq(1.12) is monotonously increasing and also convex. Then, the following relationship

$$\mathcal{E}(\mathcal{C}(\rho)) = \inf \mathcal{E}\left(\sum_i p_i \mathcal{C}(\Psi_i) \right) \leq \inf \sum_i p_i \mathcal{E}(\mathcal{C}(\Psi)) = E_F(\rho) \tag{1.14}$$

establishes that $\mathcal{E}(\mathcal{C}(\Psi))$ is an inferior limit of $E_F(\rho)$.

We introduce, now, two important features of the concurrence. First, the analytic solution to this minimization procedure involves finding the eigenvalues of the non-Hermitian operator $\rho\widetilde{\rho}$ introduced in Eq(1.11). Specifically, the closed form solution for the concurrence of a mixed state of two qubits is given by

$$\mathcal{C}(\rho) = \max\{0, \lambda_1 - \lambda_2 - \lambda_3 - \lambda_4\} \tag{1.15}$$

where the λ_i's are the square roots of the eigenvalues of $\rho\widetilde{\rho}$ and are ordered in decreasing order [9].

Further, since there always exists an optimal decomposition of ρ for a pair of qubits in which all of the pure states comprising the decomposition have the same entanglement, Wootters was able to show that we can consider the Eq(1.14) as an equality getting a closed-form for the entanglement of formation

$$E_F(\rho) = \mathcal{E}(\mathcal{C}(\rho))$$

1.4 Conclusive remarks

In this chapter we have defined the entanglement in a direct way as a non-local quantum correlation. So that, it cannot be created locally (but only globally) acting on the parties of a composed system. This is also true when the local operators are coordinated between each other (LOOC monotonicity).

We have assumed therefore that the entanglement describes those features of a quantum state which cannot be gotten separately by analyzing its parties. In other words, we will say that the entanglement is that part of the 'information' encoded in a quantum state not available locally, but obtainable only by analyzing the non-local (global) correlations.

Finally, we have introduced and discussed two measures of entanglement, and one of these, the concurrence, will be the one we will consider in the our research work reported in the following chapters.

Chapter 2

Decoherence

In this chapter we review the fundamental concept of environment induced decoherence in its various aspects, and briefly outline its crucial role in the dynamics of open entangled systems.

Firstly, we give a general overview to point out the relevance of decoherence, inevitably appearing whenever a given quantum system is coupled to its environment. In this framework, the basic ideas and formalism of decoherence are introduced, focusing the attention on the loss of *quantumness* as an effect of the surrounding environment that tends to destroy dynamically the quantum coherences.

In sec. (2.2), density operator formalism is introduced as key tool to formally describe the decoherence. Subsequently, in sec. (2.3) we show how the system-environment interaction leading to quantum decoherence may be expressed in the form of a standard von Neumann measurement scheme. Other basic concepts such as dynamical selection of a preferred basis, the decoherence function and time, and the possible emergence of decoherence-free subspace are described in sec.(2.4).

Finally, in sec.(2.5), we discuss extensively a particular pathway of two-body decoherence called Entanglement Sudden Death and review recent progress to understanding this surprising phenomenon.

2.1 Overview

In the last decade, emergent quantum technologies allowed for the experimental verification of essentially quantum effects like entanglement in mesoscopic system. Therefore, an understanding of the mechanism causing decoherence, particularly at mesoscopic scale, has become a crucial point not only in the realm of fundamental Quantum Mechanics, but also for technological purposes.

In quantum physics, decoherence is a process that implies the degradation of the purity of a quantum state, which rapidly evolves towards the corresponding classical mixture by losing the interference features. Quantum coherence, and so the capability of interference due to phase relations between the superposition-state components of a quantum system, are at the origin of various types of nonclassical properties that may be manifested in both single- and multi-partite system. In particular, quantum coherence can give rise to strong correlations between the parts of a multipartite system, called entanglement, which is an intrinsically quantum effect that cannot be explained by classical theory [1, 2].

In the first paper that introduced the main concepts of decoherence [18], Zeh pointed out that realistic quantum systems are immersed in the surrounding environment and interact inevitably with it, so that the coupling prevents the system from being isolated. The evolution of such system, called *open quantum system*, presents non-unitary features like decoherence and dissipation [19], thus quantum coherence

becomes degraded with time. Quantum decoherence, in particular, is a purely quantum effect understandable as a result of the creation of quantum correlations between the system and the its environment due to their interaction. At the same time, quantum coherence, a measure for the "quantumness" of the system, is delocalized into the entangled system-environment state. Since the state of the environment is generally inaccessible to the observer, the accompanying delocalization of phases then locally destroys superpositions between macroscopically different states, so that the reduced system appears to be in one or another of those states corresponding to its "classical" properties. This process is usually irreversible due to the large number degrees of freedom of the environment and constitutes a key component in explaining how the classical world emerges from the quantum domain.

Therefore, the decoherence properties of entangled states play a central role to explain one of the greatest foundational problems of quantum mechanics the so-called quantum-to-classical transition [20]. This issue is at the heart of the Schrödinger's cat paradox [21], which is based on entanglement between a microscopic and a macroscopic system in terms (a cat put in a quantum superposition of alive and dead states correlated with the state of a decaying atom). But it was considered a mere *Gedankenexperiment*,i.e., a thought experiment, that would play no significant role in the macroscopic world, until the 1980s when it was proposed [22, 23, 24, 25] that a macroscopic system could manifest quantum behavior, provided the coupling with the environment be weak enough.

From this point of view, the decoherence changes the nature of the quantum system itself, and the system-environment interactions in the quantum physics are not only viewed as a kind of disturbance that perturbs the system of interest that ought

to be minimized in order to properly describe the physics of this system. Instead, the coupling to the environment now defines the observable physical properties of the system. Only very special cases of typically microscopic phenomena (in the atomic realm) are described to a good degree by the isolated-system approximation so that coherent superposition of distinct physical states as predicted by quantum mechanics can actually be observed.

The first works that recognize the crucial importance of system-environment interactions and entanglement to the appearance of decoherence were in the 1970s and 1980s [18, 26, 27, 28, 29, 30]. Zurek's work has given several important contributions to the understanding of decoherence. Among these he developed the concept of environment-induced superselection and "pointer states" [29, 30] and derived a quite general and simple expression from which typical decoherence timescale could be evaluated [31]. It turned out that this process can be extremely fast, especially at macroscopic scales. In general, the effect of decoherence increases with the size of the system (from microscopic to macroscopic scales), so that, larger systems lose coherence more quickly. However, in some cases the decohering influence of the environment can be sufficiently shielded to lead to mesoscopic and even macroscopic superpositions. For example, superpositions of macroscopic currents become observable in superconducting quantum interference devices (SQUIDs) [32, 33].

Interest for decoherence was originally concerned with the consequences for quantum measurement and the quantum-classical transition. More recently, decoherence has been intended as the obstacles to circumvent to realize quantum information processing and communication schemes. This is especially the case for entangled systems. In other words, due to decoherence the system loses its ability to maintain and

exploit entanglement, and thus it becomes useless for all the applications relying on it, such as quantum cryptography and quantum computation. [34]. From this point of view, the decoherence appears as a key obstacle to next-generation technologies, such as quantum computer. Due to this practical importance, decoherence dynamics of entangled quantum systems (due to the interaction with internal or external noise sources) have been studied in different contexts involving atoms, ions, photons, quantum dots, Josephson junctions, and so on.

In particular, the most fundamental aspects of quantum coherence and decoherence can be deeply investigated in cavity QED experiments, which present the great advantage that can be described by elementary models, being at the same time rich enough to reveal intriguing subtleties of the interplay of coherent dynamics with external coupling. Cavity QED provides therefore a unique paradigm for matching theory with experiment in the study of quantum coherence, entanglement properties and monitoring of the decoherence dynamics. In this area, the experiments realized by Haroche's group [35, 36] have investigated the rapid decay of coherence of a quantum superposition of coherent states, by monitoring the decoherence dynamics.

The dominant source of decoherence in cavity QED systems is simply related to the escape of photons, due to the non-perfect reflectivity of the cavity mirrors. This can be described through a linear coupling of the cavity field to the external electromagnetic modes, constituting a reservoir of harmonic oscillators. Further, a detailed analytical description of the competition between atom-field and field environment couplings can be given in terms of an open Jaynes-Cummings model.

Decoherence of bipartite systems

The decoherence of entangled systems has started to be investigated only very recently. For such a case, one is interested in following the time evolution of the entanglement, which is lost because of the interaction of the subsystems with their (local, or common) environments. Even for the simplest entangled systems, composed of just two qubits, for which the entanglement can be efficiently evaluated using the concurrence [9], it has been shown that entanglement decoherence shows amazing dynamical features [37, 38, 39], which don't occur for the decoherence dynamics of a single system. It has been demonstrated that decoherence degrades the nonlocal (bipartite) entanglement in a very different way compared to the usual (one-body) local quantum coherence measured by the decay of off-diagonal elements of the density matrix of either qubit separately.

In particular, Yu and Eberly showed [38, 40] that an entangled system of two qubits interacting with independent environments loses entanglement abruptly after a finite time, while quantum coherences decay smoothly to zero in an infinite time. The experiment of Almeida et al. [37] gives the first confirmation of the existence of such an effect that is called *entanglement sudden death* (ESD).

Finally, we emphasize that decoherence dynamics of two independent qubits each coupled to its own environment presents new amazing features among known relaxation effects because it has no lifetime in any usual sense, that is, entanglement terminates completely after a finite interval, without a smoothly diminishing long-time tail.

As the entanglement is a key resource of quantum information, the finite time disentanglement is clearly an unwanted effect. It is known that some two-qubit states

are more robust against evolution to sudden death than others [41]. It is thus important to study the decoherence of entanglement in order to find ways of circumventing it.

Further, considerable effort has been devoted to designing strategies able to counteract the effects of environmental couplings in open-system evolutions. In particular, the effects of decoherence can adequately be controlled through sophisticated methods such as quantum error correction, decoherence-free subspaces, quantum Zeno effect, and environment engineering.

2.2 Basic concepts about decoherence in terms of density operator

We start now a more formal description of decoherence, by noticing that it derives from the possibility to divide the universe into "system" and "environment", where the term environment is usually understood as the "remainder" of the system, whose degrees of freedom are typically not controlled.

In this picture the reduced density operator is a key tool to formally describe the decoherence. The main reason for this is that the environment get rapidly entangled with the system, thus preventing the description of the latter by a pure state (indeed, it is impossible to assign an individual quantum state vector to the two sub-systems: this is the heart of the key concept of quantum non-separability). A density operator is needed, then, obtained by tracing out the unobserved degrees of freedom of the environment, and providing an elegant method to represent the measurement statistics for the system.

We can introduce a mixed-state density operator that completely encodes all statistical properties of the system. This density matrix is given by

$$\rho_m = \sum_j p_j |\phi_j\rangle\langle\phi_j| \tag{2.1}$$

with $p_j \geq 0$ and $\sum_j p_j = 1$, that can be viewed as a classical probability distribution of pure-state density operator $\rho_j = |\psi_j\rangle\langle\psi_j|$.

A mixed state expresses insufficient information about the state of the system, in the sense that the system is (before the measurement) in one of the pure states $|\phi_j\rangle$ but the observer simply does not know in which one. Therefore we can only ascribe probabilities $p_j \geq 0$ to each of the states $|\phi_j\rangle$. Such a situation typically arises if the physical procedure used to prepare a quantum state contains a probabilistic element.

We emphasize that the states $|\phi_j\rangle$ involved in ρ need not for a basis nor be orthogonal, and furthermore, even if they were a basis, a mixed state must be clearly distinguished from a pure-state superposition of the form

$$|\psi\rangle = \sum_j \sqrt{p_j}|\phi_j\rangle \tag{2.2}$$

Here all component states $|\phi_j\rangle$ are simultaneously present due to encoded maximum knowledge about the system, thus there is no a priori probabilistic element contained in this superposition. The density operator for such a state would correspond to the superposition (2.2) is

$$\begin{aligned} \rho_p = |\psi\rangle\langle\psi| &= \sum_{j,k} \sqrt{p_j p_k}|\phi_j\rangle\langle\phi_k| \\ &= \rho_m + \sum_{j\neq k} \sqrt{p_j p_k}|\phi_j\rangle\langle\phi_k| \end{aligned} \tag{2.3}$$

The off-diagonal terms in Eq(2.3), contain definite phase relations between the different superposition components of Eq(2.2), and define the quantum coherences associated with the quantum state $|\psi\rangle$ and clearly make the physical distinction between this pure-state density operator and the mixed-state density operator of Eq(2.1).

Usually, an observer will perform measurements only on the system of interest described by a reduced density matrix that is necessarily non-pure due to the presence of system-environment entanglement. As a result, the quantum coherence turns out to be extremely fragile, and can be strongly suppressed as time goes on, so that the quantum superpositions are continuously reduced to classical probability distributions.

2.3 Environment-induced decoherence

We introduce the basic formalism of decoherence, by regarding decoherence as a consequence of a von Neumann-type measurement interaction [42] between the system and its environment. Here, the environment plays the role of the quantum probe.

Such interactions induce quantum correlations between system and its environment and allow us to immediately infer certain states as the preferred states of the system that are most robust under the influence of the environment. For the reduced density matrix in a specific basis representation, the quantum coherences result to be damped on an extremely short time scale.

The hamiltonian for the total system may be decomposed into the three relevant parts

$$H = H_S + H_E + H_{int} \tag{2.4}$$

where H_S and H_E describe the intrinsic dynamics of the system and environment, respectively, and H_{int} is the system-environment interaction Hamiltonian.

The interaction Hamiltonian is taken be of the von Neumann form

$$H_{int} = \sum_n S_n \otimes E_n \tag{2.5}$$

where E_n are arbitrary operator acting only in the Hilbert space of the environment, the projector $S_n = |n\rangle\langle n|$ represents the physical quantity that is directly monitored by the environment and selects a specific set of orthonormal basis vectors $|n\rangle$ of the system.

We assume that such basis states $|n\rangle$ are not affected by the coupled dynamics due to negligible feedback of the environment on them. We may also equivalently express such condition in terms of system observables, which are simply linear combinations of the projectors $|n\rangle\langle n|$,

$$O_S = \sum_n o_n |n\rangle\langle n| \tag{2.6}$$

Thus, if the basis states $|n\rangle$ are eigenstates of H_{int}, it follows that $|n\rangle\langle n|$ and therefore also O_S commutes with H_{int}

$$[O_S, H_{int}] = 0 \tag{2.7}$$

This important condition, called *stability criterion*, was first introduced by Zurek [29, 30] and as we will see it allows to determine an preferred set of states.

Furthermore, if the projector $S_n = |n\rangle\langle n|$ commutes with the system Hamiltonian H_s, then the mean energy of the system is constant in time.

Now, we consider what happens if the system is in an initial superposition of these basis states $\sum_n c_n |n\rangle$.

In this case, the linearity of the Schrödinger equation implies that, when the initial

state of the total system is written as

$$|\Psi(0)\rangle = \sum_n c_n |n\rangle \otimes |\phi\rangle \tag{2.8}$$

where $|\phi\rangle$ is an arbitrary reservoir state (it can always be chosen as a pure state, by eventually enlarging the environmental Hilbert space), it evolves into

$$|\Psi(t)\rangle = \sum_n c_n |n\rangle \otimes |\phi_n(t)\rangle \tag{2.9}$$

where

$$|\phi_n(t)\rangle = T_{\leftarrow} e^{-i\int_0^t ds E_n(s)} |\phi\rangle \equiv V_n(t)|\phi\rangle \tag{2.10}$$

This dynamical system-environment evolution represents the ideal von Neumann quantum-measurement scheme and constitutes the basic formal representation of the decoherence process, and we shall now discuss its consequences.

Note that Eq. (2.9) shows that the system-environment interaction has established a one-to-one quantum correlation between the various system state $|n\rangle$ and corresponding environment states $|\phi_n(t)\rangle$. Thus, the final state of the system-environment combination is in general described by an entangled state given by a superposition of the states $|n\rangle \otimes |\phi_n(t)\rangle$, which has been created dynamically.

The superposition initially confined to the system state has now spread to the larger system-environment state, in the sense that the final superposition involves both the system and the environment.

Correspondingly, coherence is no longer a property of the system alone, but it has become a shared property of the global system-environment state, in a sentence: coherence has been "delocalized into the larger system", which now includes the environment.

Note that Eq (2.9) also implies that the environment carries information on the system state due to the measurement-type interaction in which the environment behaves as a probe. In this way, an irreversible flow of information occurs from the system into the environment.

However, provided that the environment has not recorded sufficient information we cannot assume that the basis vectors $|\phi_n(t)\rangle$ of the environment are mutually orthogonal, so that the coherences will be still present in the reduced density matrix of the system for the state (2.9) which is given by

$$\rho_S(t) = \mathrm{tr}_E\left[|\Psi(t)\rangle\langle\Psi(t)|\right] = \sum_{n,m} c_n c_m^* |n\rangle\langle m|\langle\phi_m(t)|\phi_n(t)\rangle \tag{2.11}$$

obtained by tracing out the unobserved degrees of the environment.

It follows from unitarity that $\langle\phi_n(t)|\phi_n(t)\rangle = 1$, so that, the populations don't decay. While, in general, the coherences, that describe the interference between the superposition-state components $|n\rangle$ of the system, are often found to be rapidly decaying.

The time dependence of the matrix element $\langle n|\rho_S(t)|m\rangle$ is expressed in terms of the corresponding environment states as follow

$$|\langle\phi_n(t)|\phi_m(t)\rangle| = e^{\Gamma_{nm}}\,, \qquad \Gamma_{nm} \leq 0 \tag{2.12}$$

where Γ_{nm}, for $n \neq m$, describes the behavior of the off-diagonal elements of $\rho_S(t)$ and is called *decoherence function.*

Note that the time dependence of the decoherence function Γ_{nm} is determined by the time evolution of the environmental states, so that it depends on the specific modelling of system-environment interactions.

Typically, for many system-environment models, the irreversible dynamics induced by the system-environment interaction leads to an exponential decay of the overlap of the different relative environment states $|\phi_n(t)\rangle$ as follows

$$|\langle\phi_n(t)|\phi_m(t)\rangle| \propto e^{-t/\tau_D}\,, \qquad \text{for} \quad n \neq m \tag{2.13}$$

where τ_D denotes the characteristic decoherence time scale, which is the delay required for the relative environment states $|\phi_n(t)\rangle$ to becomes orthogonal.

Many explicit physical models for the interaction of a system with the environment, however, have shown that due to the large number of freedom degrees of the environment, the environment states $|\psi_n(t)\rangle$ rapidly approach orthogonality,

$$\langle\phi_n(t)|\phi_m(t)\rangle \to \delta_{nm}\,, \qquad \text{for} \quad t \gg \tau_D. \tag{2.14}$$

Detailed models, in which the environment is typically represented by a reservoir of harmonic oscillators [43, 44, 45, 46, 47, 48], have shown that the damping occurs on extremely short decoherence time scales τ_D, which are typically many orders of magnitude shorter than the thermal relaxation.

Thus, the reduced density matrix $\rho_S(t)$ becomes diagonal in the preferred basis $\{|n\rangle\}$, that is,

$$\rho_S(t) \to \sum_n |c_n|^2\, |n\rangle\langle n|\,, \qquad \text{for} \quad t \gg \tau_D \tag{2.15}$$

Note that these basis states are selected by the form of the system-environment interaction (2.5) and by the behavior of the decoherence function embodied in (2.14), so that can be viewed as a consequence of the decoherence process.

The preferred states of the system emerge dynamically as those states that survive the environment selection being the most robust to the interaction with the environment, in the sense that they become least entangled with the environment in the

course of the evolution and are thus most immune to decoherence. W. Zurek has compared this process of decoherence to a Darwinian process ensuring the "survival of the fittest" [47].

Moreover, the interference terms of the density matrix have vanished in this basis due to system-environment interaction. In other words, the pure state of the reduced system S becomes a mixture, so that the phase relation between the components in the superposition of the pure state, and so the coherence, i.e., the capability of interference, are lost for S.

This practically irreversible environment-induced delocalization of phase relations into the composite system-environment state expressed by (2.15) constitutes the process of decoherence.

Only measurements that include both the system and the environment could reveal the coherence between the components in the superposition state (2.9). However, in practice, it is impossible to include in our observation all the many environmental degrees of freedom that have interacted with the system and in which the quantum coherence is distributed. That is, the interference terms remain present at the global level of the system-environment superposition (2.9) but have become unobservable at the local level of the system as described by the reduced density matrix (2.15).

Finally, we can state that all physical systems are open quantum systems that interact with their environment, so that the environment continuously acquires information about the system, leading to a constant 'leakage' of coherence from the system into the environment.

The decoherence process described here is a purely quantum effect, related to entanglement with the environment. Nevertheless, a quantum system can lose its

quantum coherence in a purely classical way related to random disturbances of the relative phases of a quantum state due to fluctuations of classical quantities. Moreover, there is no energy exchange between the system and its environment.

Most generally, the system can be in the state

$$|\psi\rangle = \sum_j \alpha_j e^{i\phi_j(t)} |\psi_j\rangle$$

where $\phi_j(t)$ are classical random functions of t, called *phase noise*, due to "classical environment noise" which affects the system and its evolution, without involving entanglement with the environment. This classical process of quantum phase diffusion is called "noise induced dephasing" to distinguish it from the quantum decoherence.

Restoring the coherence is much more complicated in the case of a quantum environment because, contrary to a classical noise source, it is entangled to the system and its different parts are strongly entangled with each other. Thus the decoherence process is inherently irreversible, whereas classical noise is inherently reversible (although, in practise, not easily reverted).

2.4 Decoherence-free subspace

It is known that entangled states evolve differently under different environmental influences if special symmetries exist, so that there may exist decoherence-free subspaces in which the entangled states are well protected against interaction with the environment.

In the previous section we have seen that a preferred set of states of the system exists, which are most robust under the influence of the environment and are also the eigenstates of the interaction Hamiltonian.

Let us consider again an interaction of the form (2.5), that, if S_n are Hermitian, describes the simultaneous environment monitoring of different observables S_n on the system. Now, we show as the condition (2.7) for stability criterion can be extended to select certain subspaces in which the coherences are observable locally. These are called *decoherence-free subspaces*, and were first introduced by Zurek in 1982 [30] and recently further explored with the purpose to protect the entanglement [49, 50, 51, 52]. In particular, the preferred states $|nj\rangle$ defined by the requirement (2.7) must form an orthonormal basis $\{|nj\rangle\}$ of the subspace, and all $|nj\rangle$ must be simultaneous degenerate eigenstates of each S_n.

In this way, we can define the operator S_n as follows

$$S_n = \sum_{j}^{d_n} |nj\rangle\langle nj| \tag{2.16}$$

which singles out an orthogonal decomposition of the system's state space $\mathcal{H}_S$ into linear subspace $S_n\mathcal{H}_S$ of dimensions d_n.

Then the time evolution of the initial state written as

$$|\Psi(0)\rangle = \sum_{n,j} c_{nj}|nj\rangle \otimes |\phi\rangle \tag{2.17}$$

yields the reduced density matrix

$$\rho_S(t) = \mathrm{tr}_E\left[|\Psi(t)\rangle\langle\Psi(t)|\right] = \sum_{n,m}\sum_{jj'} c_{nj}c^*_{mj'}|nj\rangle\langle mj'|\langle\phi_m(t)|\phi_n(t)\rangle. \tag{2.18}$$

Under the condition of complete decoherence expressed by (2.14) this becomes

$$\rho_S(t) \to \sum_{n}\sum_{jj'} c_{nj}c^*_{nj'}|nj\rangle\langle nj'|\,, \qquad \text{for} \quad t \gg \tau_D \tag{2.19}$$

One can see that off-diagonal elements of the density matrix are not suppressed; thus the coherences, and so the capability of interference, are still present between

the basis states $|nj\rangle$ for different j and fixed n, which span a subspace $S_n\mathcal{H}_S$ immune to decoherence.

Then the Hilbert space of the system can be orthogonally decomposed into coherent subspaces $S_n\mathcal{H}_S$ as follow

$$\mathcal{H}_S = \sum_n S_n\mathcal{H}_S \tag{2.20}$$

so that any state of one subspace can be expressed as a superposition of the basis states $|nj\rangle$, spanning such subspace, and the coherence between the superposition-state components survive to decoherence because this state does not become entangled with the environment. Whereas the coherence between different subspaces are locally suppressed.

Moreover, we notice that one needs to ensure that the subspace remains decoherence-free over time under the action of H_S. That is, we will need to demand that none of the basis states $|nj\rangle$ of the coherent subspace will drift out of the subspace under the evolution generated by H_S. Otherwise an initially decoherence-free state would in general be affected by decoherence. In other words, H_S must not project any of the basis states $|nj\rangle$ into a Hilbert subspace outside of the subspace spanned by the basis $\{|nj\rangle\}$.

In this case, if the system starts out in a state within a coherent subspace and if it has no correlations with the environment, the system-environment state will remain in a separable state at all times. Indeed, the system does not get entangled with its environment, and thus no decoherence occurs.

We must notice that, although the stability criterion (2.7) is a conceptually intuitive methods for determining the most robust states when quantum-measurement limit holds, it is often not adequate in more complex situations.

Therefore more general methods were developed by Zurek [53, 54] and Zurek, Habib, and Paz [48] under the name of the *predictability-sieve* strategy. The basic idea consists of using a suitable measure for the amount of decoherence introduced into the system, such as the purity or the von Neumann entropy of the reduced density matrix. The states most immune to decoherence will be those which lead to the smallest decrease in purity or the smallest increase in von Neumann entropy.

2.5 Entanglement sudden death - ESD

It is well known that the loss of entanglement cannot be restored by local operations and classical communications (LOOC), therefore it becomes an important subject to study entanglement dynamics of systems subject to decoherence and to conceive methods to protect the entanglement.

In the previous sections we have seen that the local coherence (one-body) decays asymptotically to zero after an infinite time due to environment-induced decoherence, and this behavior leads to the identification of the coherence lifetime.

Recently, it has been shown that entanglement of two independent qubits each coupled to its own environment is lost in a very different way. The presence of either pure vacuum noise or even classical noise can cause entanglement to decay abruptly to zero in a finite time [38, 40, 55], an effect that is called *entanglement sudden death* (ESD).

An example of the ESD phenomenon is provided by the weakly dissipative process of spontaneous emission, and we consider a class of bipartite mixed states, called X states, and their time evolution in the presence of common pure vacuum noise.

This X mixed state arises naturally in a wide variety of physical situations [56, 57,

58]. We particularly note that it includes pure Bell states as well as the well-known Werner mixed state [59] as special cases.

In order to describe the dynamic evolution of quantum entanglement, the concurrence $\mathcal{C}(t)$ [9]is used evaluated starting from the two-qubit state at time t. In particular, for an initial state of the form $|\Phi\rangle = \alpha|00\rangle + \beta|11\rangle$, the concurrence is given by

$$\mathcal{C}(t) = \max\left\{0,\, 2e^{-\gamma t}\,|\beta|\,\left[|\alpha| - \left(1 - e^{-\gamma t}\right)|\beta|\right]\right\}$$

where γ is the vacuum emission rate of the excited atomic state. Moreover, one can see that the entanglement behavior depends on the relation between $|\alpha|$ and $|\beta|$ [55], and for $|\beta| \leq |\alpha|$ entanglement asymptotically decays to zero. Whereas for $|\beta| > |\alpha|$, entanglement disappears at finite time

$$\bar{t} = -\frac{1}{\gamma}\ln\left(1 - \frac{|\alpha|}{|\beta|}\right)$$

Differently, two-qubit states of the form $|\Psi\rangle = \alpha|01\rangle + \beta|10\rangle$ exhibit disentanglement only asymptotically in time.

Thus, the appearance of ESD depends on the amount of the initial probability for the two qubits to be in the doubly excited state $|11\rangle$

This finite-time decoherence is a new form of decay induced by classical as well as quantum noises that affects only two-qubit entanglement [60, 40], and unknown among dissipation effects of other physical correlations. Further, ESD can be provided by the weakly dissipative process of spontaneous emission, that obeys the half-life rule rigorously for individual atoms, whereas, in counterintuitive way, two-qubit entanglement does not follow the same decay rule.

Entanglement sudden death has already been experimentally proved in two different contexts. The experiment of Almeida et al. [37] gives the first confirmation to

the existence of a such effect by using an all optical setup with polarization entangled photons, whereas the experimental setup of Laurat et al. [61] exploited two separate caesium atomic ensembles in a magneto-optical trap.

Decoherence may arise in many different situations whenever the system of interest is not completely isolated from its environments. In particular, different types of environmental noise can have different effects on two-body entanglement [60], as it has been verified from Almeida et al. that have examined a two-qubit system coupled to external sources of phase-damping and amplitude-damping noises. Typically, *amplitude decoherence*, caused by spontaneous emissions of atoms, is in a sense more destructive than *phase decay*, caused by random disturbances of the relative phases of a quantum state, because the former causes diagonal and off-diagonal relaxation and the latter off-diagonal relaxation alone.

These different behaviors of entanglement decay can be seen by examining the entanglement evolution for X-states with void probability that both qubits are in their ground states. When amplitude and phase noises are applied separately ESD occurs only for some X-states affected by amplitude noise, so that infinitely long smooth decay of entanglement is allowed. Whereas, the combined effect of the two noises causes always ESD.

Another crucial result to understanding the two-body decoherence emerges in an idealized double Jaynes-Cummings model similar to previous scenario manifesting ESD but in which the cavities are lossless. Indeed, the qubits A and B, being non-interacting and non-communicating, can abruptly lose their entanglement while they interact with their own cavity fields. Thus, in this case, ESD occurs also without the "traditional" decoherence (lossless cavities are as far from being standard decoherence

reservoirs as possible).

Further, given the lossless nature of the evolution, one can expect that the entanglement can be suddenly re-generated, a process called entanglement sudden birth [62, 63]. Indeed, the original entanglement value is found to reappear in a periodic way following each sudden death event.

Finally, we note that the disappearance of two-qubit entanglement is due to a leakage of information about the qubit system towards the cavity modes. On the other hand, the lost information will come back to the qubit systems in finite times due to a memory effect of the cavities. Thus, this idealized model provides a convenient framework to analyze entanglement in a simplified framework with many qubits.

However, there is still no deep understanding of sudden death dynamics, and so far there is no known way to avoid ESD. This effect is so rapid and complete that the decay cannot be reversed using the error-correction schemes that have been proposed to increase the lifetimes of entangled qubits with a gradual nature of the decay. Further, for this two-qubit model the environment influences each qubit independently, so there are no decoherence-free subspaces and there is no such protection from ESD available. It could be possible to avoid sudden death only by using appropriate local initial preparations.

Chapter 3

Quantum entanglement and its dynamics in a lossy cavity

3.1 Introduction

Quantum entanglement is the powerful resource lying at the root of a new class of technologies based on the laws of quantum theory. The coherent manipulation of quantum systems involves very delicate procedures since the inevitable interaction with their surroundings leads to a loss of information that causes both the transformation of quantum superposition into statistical mixtures, a process called decoherence, and the disappearance of quantum entanglement in composite systems.

Recently, it has been shown that entanglement can be lost completely in a finite time despite the fact that complete decoherence only occurs asymptotically. This phenomenon, named entanglement sudden death, has been theoretically predicted by Yu and Eberly [38, 60, 64], and experimentally observed for entangled photon pairs [37] and atomic ensembles [61]. Typically, entanglement sudden death occurs when the two qubits interact with two independent environments as for the case, e.g., of two entangled qubits placed inside two different cavities. For such a configuration, a

class of states has been identified which do not experience a complete entanglement loss despite the interaction with local vacuum environments [65]. However, for finite temperature environments the sudden death occurs almost independently of the initial state of the qubit pair [66], although with details that can depend on the amount of non-Markovianity of the environments [67, 68]. In this context, a deeper understanding of the sudden death process has been gained by looking at the quantum correlations shared by the environments which show a sudden birth (though with a quite counterintuitive timing) [69, 63].

A completely different phenomenology emerges when the qubits interact with the same environment. In this case, indeed, entanglement can be created starting from a factorized state or it can even revive after a sudden death. This is due to the effective qubit-qubit interaction mediated by the common reservoir [70, 71, 72, 73, 74, 75, 76, ?, 77]. Many theoretical papers have studied reservoir-induced entanglement in the Markovian regime, that is when the coupling between the qubits and the environment is weak enough to neglect the feedback of information from the reservoir into the system (memoryless dynamics). An interesting extension to these approaches, that goes beyond the Born-Markov approximation, has been presented in Ref. [78]. Besides, it is well known [49, 79, 80] that the interaction with a *common* environment leads to the existence of a highly entangled long-living decoherence-free (or sub-radiant) state. At the same time, another entangled state exists (orthogonal to previous one and called super-radiant) that looses its coherence faster.

Here we extend these results to a dissipative coupling with the environment outside the Markovian regime, both for weak and strong couplings, corresponding to the bad and good cavity limits. In particular, in the latter regime, the long memory of the

reservoir induces entanglement revivals and oscillations.

Specifically, we address an exactly solvable non-Markovian model describing two two-level atoms (qubits) resonantly coupled to a common structured environment (lossy resonator) using an exact approach that does not rely on the Born-Markov approximation [81].

As we discuss below, this describes, e.g., atoms or ions trapped in an electromagnetic cavity [82, 83] or circuit-QED setups[84, 85, 86] and our results are directly verifiable in both systems.

First, we focused on the case in which the qubits were identical and resonant with the cavity field, whose spectrum was modeled as a Lorentzian. We obtain the exact entanglement dynamics as a function of the environment correlation time and discuss its stationary value, which turns out to be maximal for a factorized initial state of the two atoms.

Besides, we extend our analytical approach to describe the more general situation in which the qubit frequencies are different and non-resonant with the main mode supported by the cavity.

Our new analytical results allow us to characterize completely and exactly the entanglement dynamics for a generic initial two-qubit state containing one excitation. We study the time evolution of the entanglement and its dependence on several parameters, all in principle adjustable in the experiments: the relative coupling between the atoms and the cavity field, the initial amount of entanglement, the frequency of the qubits, the detuning from the cavity field, and the quality factor of the cavity. In this way we determine the conditions to achieve maximal reservoir-induced entanglement generation for an initial factorized state of the qubits, and to minimize the loss

of entanglement for an initial entangled state.

Depending on the matching of the qubit frequencies, we will distinguish two scenarios displaying different qualitative long time behavior. If the two qubits have the same transition frequency ($\omega_1 = \omega_2$), a decoherence-free state (subradiant state) exists [49, 79, 80]. Due to the presence of such a dark state, a non-zero asymptotic entanglement can be obtained in this case. On the other hand, if the two qubits have different transition frequencies ($\omega_1 \neq \omega_2$), no subradiant state exists, so that the stationary entanglement always vanishes. For the sake of brevity, we refer to these two cases as subradiant and non-subradiant scenario, respectively.

One of our main results is the demonstration that high values of reservoir-induced entanglement can be obtained in the dispersive regime even in the bad cavity limit. In general, in this regime the dynamics of the concurrence (that we employ to quantify entanglement [9]) is characterized by a quasi-regular and quasi-periodical pattern since the cavity photon is only virtually excited and therefore the two-qubit system is less affected by the cavity losses. Finally, in the good cavity limit, we predict the occurrence of quantum beats of entanglement and explain their physical origin.

The chapter is structured as follows.

In Sec. 3.2 we present the microscopic Hamiltonian model, for which the exact analytical solution is presented, where we focus on the case in which the spectrum of the environment is Lorentzian as, e.g., for the electromagnetic field inside a lossy resonator.

In Sec. 3.3 we introduce the entanglement dynamics , in particular, in Sec. 3.4, 3.5 and 3.6 we present and discuss our main results by looking at the entanglement dynamics in the resonant regime, and both off-resonant subradiant and non-subradiant

scenarios, respectively, for different coupling regimes and different initial states.

Finally, Sec. 3.7 contains summary and conclusions.

3.2 The model

We study an open quantum system consisting of two qubits coupled to a common zero-temperature bosonic reservoir in the vacuum. The Hamiltonian describing the total system is given by

$$H = H_S + H_R + H_{\rm int}, \tag{3.1}$$

where H_S is the Hamiltonian of the qubits system coupled, via the interaction Hamiltonian $H_{\rm int}$, to the common reservoir, whose Hamiltonian is H_R.

The Hamiltonian for the total system, in the dipole and the rotating-wave approximations, can be written as (assuming $\hbar = 1$)

$$\begin{aligned} H_S &= \omega_1 \sigma_+^{(1)} \sigma_-^{(1)} + \omega_2 \sigma_+^{(2)} \sigma_-^{(2)}, & (3.2)\\ H_R &= \sum_k \omega_k b_k^\dagger b_k, & (3.3)\\ H_{\rm int} &= \left(\alpha_1 \sigma_+^{(1)} + \alpha_2 \sigma_+^{(2)}\right) \sum_k g_k b_k + \text{h.c.}, & (3.4) \end{aligned}$$

where $b_k^\dagger$, b_k are the creation and annihilation operators of quanta of the reservoir, $\sigma_\pm^{(j)}$ and ω_j are the inversion operators and transition frequency of the j-th qubit ($j = 1, 2$); finally ω_k and $\alpha_j g_k$ are the frequency of the mode k of the reservoir and its coupling strength with the j-th qubit.

Here, the α's are dimensionless real coupling constants measuring the interaction strength of each single qubit with the reservoir. In particular, we assume that these two constants can be varied independently. In the case of two atoms inside a cavity,

e.g., this can be achieved by changing the relative position of the atoms in the cavity field standing wave. For the following discussion, it will prove useful to introduce a collective coupling constant $\alpha_T = (\alpha_1^2 + \alpha_2^2)^{1/2}$ and the relative strengths $r_j = \alpha_j/\alpha_T$ (as $r_1^2 + r_2^2 = 1$, we take only r_1 as independent). By varying α_T, we will explore both the weak and the strong coupling regimes.

3.2.1 Dynamics of the qubit system

We assume that initially the qubit system and the reservoir are disentangled. We restrict ourselves to the case in which only one excitation is present in the system and the reservoir is in the vacuum. In this case the initial state for the whole system can be written as

$$|\Psi(0)\rangle = \Big[c_{01}|1\rangle_1|0\rangle_2 + c_{02}|0\rangle_1|1\rangle_2\Big] \bigotimes_k |0_k\rangle_R, \tag{3.5}$$

where $|0\rangle_j$ and $|1\rangle_j$ $(j = 1, 2)$ are the ground and excited states of the j-th qubit, respectively, while $|0_k\rangle_R$ is the state of the reservoir with zero excitations in the mode k.

The time evolution of the total system, under the action of this Hamiltonian, is given by

$$\begin{aligned} |\Psi(t)\rangle &= c_1(t)|1\rangle_1|0\rangle_2|0\rangle_R + c_2(t)|0\rangle_1|1\rangle_2|0\rangle_R + \\ &\quad + \sum_k c_k(t)|0\rangle_1|0\rangle_2|1_k\rangle_R, \end{aligned} \tag{3.6}$$

where $|1_k\rangle_R$ is the state of the reservoir with only one excitation in the k-th mode and $|0\rangle_R = \bigotimes_k |0_k\rangle$.

The reduced density matrix describing the two-qubit systems, obtained from the

density operator $|\Psi(t)\rangle\langle\Psi(t)|$ after tracing over the reservoir degrees of freedom, takes the form

$$\rho(t) = \begin{pmatrix} 0 & 0 & 0 & 0 \\ 0 & |c_1(t)|^2 & c_1(t)c_2^*(t) & 0 \\ 0 & c_1^*(t)c_2(t) & |c_2(t)|^2 & 0 \\ 0 & 0 & 0 & 1-|c_1|^2-|c_2|^2 \end{pmatrix}. \tag{3.7}$$

The two-qubit dynamics is therefore completely characterized by the amplitudes $c_{1,2}(t)$.

Introducing the j-qubit detuning from the mode k, $\delta_k^{(j)} = \omega_j - \omega_k$, the equations for the probability amplitudes take the form

$$\dot{c}_j(t) = -i\alpha_j \sum_k g_k e^{i\delta_k^{(j)}t} c_k(t), \quad j = 1,2 \tag{3.8}$$

$$\dot{c}_k(t) = -ig_k^* \left[\alpha_1 e^{-i\delta_k^{(1)}t} c_1(t) + \alpha_2 e^{-i\delta_k^{(2)}t} c_2(t)\right]. \tag{3.9}$$

Formally integrating Eq. (3.9) and inserting its solution into Eqs. (3.8), one obtains two integro-differential equations for $c_{1,2}(t)$,

$$\begin{aligned} \dot{c}_1(t) = -\sum_k \int_0^t dt_1 \Big[& \alpha_1^2 |g_k|^2 e^{i\,\delta_k^{(1)}(t-t_1)} c_1(t_1) \\ & + \alpha_1\alpha_2 |g_k|^2 e^{i\,\delta_k^{(1)}t} e^{-i\,\delta_k^{(2)}t_1} c_2(t_1)\Big], \end{aligned} \tag{3.10}$$

$$\begin{aligned} \dot{c}_2(t) = -\sum_k \int_0^t dt_1 \Big[& \alpha_1\alpha_2 |g_k|^2 e^{i\,\delta_k^{(2)}t} e^{-i\,\delta_k^{(1)}t_1} c_1(t_1) \\ & + \alpha_2^2 |g_k|^2 e^{i\,\delta_k^{(2)}(t-t_1)} c_2(t_1)\Big]. \end{aligned} \tag{3.11}$$

In the continuum limit for the reservoir spectrum the sum over the modes is replaced by the integral

$$\sum_k |g_k|^2 \to \int d\omega J(\omega),$$

where $J(\omega)$ is the reservoir spectral density. In the following we focus on the case in which the structured reservoir is the electromagnetic field inside a lossy cavity. In this case, the fundamental mode supported by the cavity displays a Lorentzian broadening due to the non-perfect reflectivity of the cavity mirrors. Hence the spectrum of the field inside the cavity can be modeled as

$$J(\omega) = \frac{W^2}{\pi} \frac{\lambda}{(\omega - \omega_c)^2 + \lambda^2}, \tag{3.12}$$

where the weight W is proportional to the vacuum Rabi frequency and λ is the width of the distribution and therefore describes the cavity losses (photon escape rate).

We now introduce the correlation function $f(t - t_1)$, defined as the Fourier transform of the reservoir spectral density $J(\omega)$,

$$f(t - t_1) = \int d\omega J(\omega) e^{i(\omega_c - \omega)(t - t_1)},$$

where ω_c is the fundamental frequency of the cavity.

When the spectrum of the cavity field displays a Lorentzian broadening, the correlation function decays exponentially $f(\tau) = W^2 e^{-\lambda\tau}$, the quantity $1/\lambda$ being the reservoir correlation time. The ideal cavity limit is obtained for $\lambda \to 0$; in this case one has

$$\lim_{\lambda \to 0} J(\omega) = W^2 \delta(\omega - \omega_0), \tag{3.13}$$

corresponding to a constant correlation function $f(\tau) = W^2$. The system, then, reduces to a two-atom Jaynes-Cummings model [87] with a vacuum Rabi frequency $\mathcal{R} = \alpha_T W$. On the other hand, for small correlation times (with λ much larger than any other frequency scale), we obtain the Markovian regime characterized by a decay rate $\gamma = 2\mathcal{R}^2/\lambda$. For generic parameter values, the model interpolates between these two limits.

In terms of the correlation function Eqs. (3.10)-(3.11) become

$$\begin{aligned}\dot{c}_1(t) &= -\int_0^t dt_1 \left[\alpha_1^2\, c_1(t_1) + \alpha_1\alpha_2\, c_2(t_1) e^{-i\,\delta_{21} t_1}\right] \\ &\quad \times f(t-t_1) e^{i\,\delta_1 (t-t_1)}, \end{aligned} \tag{3.14}$$

$$\begin{aligned}\dot{c}_2(t) &= -\int_0^t dt_1 \left[\alpha_1\alpha_2\, c_1(t_1) e^{i\,\delta_{21} t_1} + \alpha_2^2\, c_2(t_1)\right] \\ &\quad \times f(t-t_1) e^{i\,\delta_2 (t-t_1)}, \end{aligned} \tag{3.15}$$

where $\delta_j = \omega_j - \omega_c$ and $\delta_{21} = \omega_2 - \omega_1$.

Performing the Laplace transform of Eqs. (3.14)-(3.15) yields

$$\begin{aligned} s\,\widetilde{c}_1(s) - c_1(0) &= -\left[\alpha_1^2\,\widetilde{c}_1(s) + \alpha_1\alpha_2\,\widetilde{c}_2(s + i\,\delta_{21})\right] \\ &\quad \times \widetilde{f}(s - i\,\delta_1), \end{aligned} \tag{3.16}$$

$$\begin{aligned} s\,\widetilde{c}_2(s) - c_2(0) &= -\left[\alpha_1\alpha_2\,\widetilde{c}_1(s - i\,\delta_{21}) + \alpha_2^2\,\widetilde{c}_2(s)\right] \\ &\quad \times \widetilde{f}(s - i\,\delta_2). \end{aligned} \tag{3.17}$$

From the equations above one can derive the quantities $\widetilde{c}_1(s)$ and $\widetilde{c}_2(s)$. Finally, inverting the Laplace transform one obtains a formal solution for the amplitudes $c_1(t)$ and $c_2(t)$. The main steps for deriving the general solution are outlined in Appendix A. For specific forms of the reservoir spectral density, as the one we consider in this paper, it is possible to obtain simple analytic expressions for these coefficients.

Before discussing the general features of the dynamics we notice that, when the two qubits have the same transition frequency, $\omega_1 = \omega_2$, a subradiant, decoherence-free state exists, that does not decay in time. The existence of the subradiant state does not depend on the form of the spectral density and therefore on the resonance/off-resonance condition. Such a state takes the form

$$|\psi_-\rangle = r_2|1\rangle_1|0\rangle_2 - r_1|0\rangle_1|1\rangle_2. \tag{3.18}$$

When the two qubits have different frequencies, $\omega_1 \neq \omega_2$, there is no decoherence-free state.

This simple consideration enables us to draw general conclusions about the dynamics of entanglement for long times. Indeed, one can observe two qualitatively different behaviors. In the subradiant scenario, occurring for $\omega_1 = \omega_2$, a subradiant state exists and therefore that part of the initial entanglement stored in $|\psi_-\rangle$ will be 'trapped' for arbitrary long times. In the non-subradiant scenario, when $\omega_1 \neq \omega_2$, the subradiant state does not exist. Hence all initial entanglement will decay and is eventually lost for long times.

We now derive the solution for the coefficients $c_1(t)$ and $c_2(t)$ and study the entanglement dynamics discussing separately the two cases outlined above.

3.2.2 Subradiant Scenario

For $\omega_1 = \omega_2$ the analytical solution for the amplitudes $c_1(t)$ and $c_2(t)$ takes a simple form, with a structure analogous to the solution of the resonant case presented in Ref. [81],

$$c_1(t) = \left[r_2^2 + r_1^2 \, \mathcal{E}(t) \right] c_1(0) - r_1 r_2 \left[1 - \mathcal{E}(t) \right] c_2(0), \tag{3.19}$$

$$c_2(t) = -r_1 r_2 \left[1 - \mathcal{E}(t) \right] c_1(0) + \left[r_1^2 + r_2^2 \, \mathcal{E}(t) \right] c_2(0), \tag{3.20}$$

with

$$\mathcal{E}(t) = e^{-(\lambda - i\delta)\, t/2} \left[\cosh\left(\Omega t/2\right) + \frac{\lambda - i\delta}{\Omega} \sinh\left(\Omega t/2\right) \right], \tag{3.21}$$

where $\delta_1 = \delta_2 \equiv \delta$ and $\Omega = \sqrt{\lambda^2 - \Omega_R^2 - i2\delta\lambda}$, with $\Omega_R = \sqrt{4W^2\alpha_T^2 + \delta^2}$ the *generalized Rabi frequency* and $\mathcal{R} = W\alpha_T$ the *vacuum Rabi frequency.*

As in the resonant case, the state $|\psi_-\rangle$ does not evolve in time and the only relevant time evolution is the one of its orthogonal superradiant state

$$|\psi_+\rangle = r_1|1\rangle_1|0\rangle_2 + r_2|0\rangle_1|1\rangle_2. \tag{3.22}$$

The function $\mathcal{E}(t)$ is the survival amplitude of the superradiant state $\langle\psi_+(t)|\psi_+(0)\rangle = \mathcal{E}(t)$. If we express the initial state of the qubits as a superposition of $|\psi_\pm\rangle$, that is $|\psi(0)\rangle = \beta_-|\psi_-\rangle + \beta_+|\psi_+\rangle$ with $\beta_\pm = \langle\psi_\pm|\,\psi(0)\rangle$, we see that, while part of the initial state will be trapped in the subradiant state $|\psi_-\rangle$, another part will decay following Eq. (3.21). Thus the amount of entanglement that survives depends on the specific initial state and on the value of the coefficients r_j.

3.2.3 Non-subradiant Scenario

For $\omega_1 \neq \omega_2$ no subradiant or decoherence-free state exists and, as a consequence, the analytical expression for the amplitudes $c_{1,2}(t)$ becomes more complicated

$$c_1(t) = \mathcal{E}_{11}(t; r_1)c_1(0) + \mathcal{E}_{12}(t; r_1)c_2(0), \tag{3.23}$$

$$c_2(t) = \mathcal{E}_{21}(t; r_1)c_1(0) + \mathcal{E}_{22}(t; r_1)c_2(0), \tag{3.24}$$

where the functions $\mathcal{E}_{ij}(t; r_1)$ depend not only on time but also on the value of r_1.

We emphasize that in both scenarios, the solution of the differential equations for the amplitudes $c_{1,2}(t)$ is exact as we have not performed neither the Born nor the Markov approximation. The structure of the functions $\mathcal{E}_{ij}(t;r_1)$ and the main steps to the solution are briefly outlined in Appendix A.

3.2.4 Dispersive regime

In this subsection we focus on the system dynamics when the qubits are far off-resonant from the main cavity mode, i.e. for $\delta_1, \delta_2 \gg \mathcal{R}$. In this regime, both in the subradiant and in the non-subradiant scenarios, the main features of the dynamics can be obtained by looking at the effective dispersive Hamiltonian describing the coupling of the two qubits with a single-mode cavity field [88, 89, 90] and remembering that this behavior must then be corrected taking into account the effect of the cavity losses. In Appendix B we derive the effective dispersive Hamiltonian for this system, assuming that the cavity field is initially in the vacuum state,

$$H_{eff} = \sum_{j=1}^{2} \frac{\mathcal{R}^2\, r_j^2}{\delta_j}\, \sigma_+^{(j)}\sigma_-^{(j)} + \frac{\mathcal{R}^2\, r_1 r_2}{2\,\delta_j} \left(\sigma_+^{(1)}\sigma_-^{(2)} + \sigma_+^{(2)}\sigma_-^{(1)}\right). \tag{3.25}$$

The first two terms in the Hamiltonian are proportional to $\sigma_+^{(j)}\sigma_-^{(j)}$ and describe the Stark shifts due to the dispersive interaction with the cavity vacuum. The remaining terms describe an effective dipole-dipole coupling between the two atoms induced by the cavity mode. As we will see in the following these two terms play an essential role in the entanglement generation process. By looking at Eq. (3.25) we notice that both the Stark shifts and the effective interaction strength between the qubits are now $\propto \mathcal{R}^2/\delta_{1,2}$.

In the dispersive regime the cavity is only virtually excited, thus the photon loss is

less important and the effective decoherence rate due to the cavity decay is strongly suppressed to the advantage of the generation of entanglement. As we will see in Sec. 3.5.1 for the subradiant scenario, the effective decoherence rate due to the cavity decay in this case becomes $(\mathcal{R}^2/\delta^2)\lambda$.

3.3 Entanglement Dynamics

To study the time evolution of the two-qubit entanglement we use the concurrence $C(t)$ [9]. This is an entanglement measure related to the entanglement of formation, ranging from one for maximally entangled states to zero for separable ones.

For the system of two qubits described by reduced density matrix of Eq. (3.7) the concurrence takes a very simple form

$$C(t) = 2\left|c_1(t)\, c_2^*(t)\right|. \tag{3.26}$$

Such equation shows a relation between the behavior of the concurrence and the time evolution of the excitation shared by the two qubits. Having in mind the considerations of Sec. 3.2.4 one may understand how, through a suitable choice of the detuning between the qubits and the cavity, it is possible to improve both the generation of entanglement and its preservation for long times.

To better discuss the time evolution of the concurrence as a function of the initial amount of entanglement stored in the system, we consider a general initial states of the form given by Eq. (3.5) with

$$c_{01} = \sqrt{\frac{1-s}{2}}, \quad c_{02} = \sqrt{\frac{1+s}{2}}\, e^{i\phi}, \text{ with } \quad -1 \leq s \leq 1.$$

Here, the separability parameter s is related to the initial concurrence as $s^2 = 1 - C(0)^2$.

Before describing in detail the dynamics in the resonant regime (Sec. 3.4) and in both off-resonant subradiant scenario (Sec. 3.5) and non-subradiant scenario (Sec. 3.6), it is useful to discuss the steady-state entanglement [81].

3.3.1 Stationary concurrence

We begin by noticing that there exist a non-zero stationary value of C due to the entanglement of the decoherence-free state: $C_s = C(t \to \infty) \equiv C(|\psi_-\rangle)\ |\langle\psi_-|\,\psi(0)\rangle|^2 = 2|r_1 r_2|\ |\beta_-|^2$.

Fig. 3.1-(a) displays the stationary concurrence versus r_1 and s. Due to the interaction with the cavity field, initial separable states ($s = \pm 1$) become entangled. In fact, for $\phi = 0$, the maximum stationary entanglement $C_s^{\max} \simeq 0.65$ is obtained for initially factorized states, i.e. $s = \pm 1$. While the details depend on the phase ϕ, the qualitative picture is generic and essentially independent of ϕ, apart from the isolated case of an initial state coinciding with $|\psi_-\rangle$. In such a situation all of the entanglement initially encoded in the qubits remains there for long times. For positive r_j, this occurs for $\phi = \pi$, see Fig. 3.1-(b).

3.4 Resonant Entanglement

We now look at the entanglement dynamics in the good and bad cavity limits, i.e. for $R \gg 1$ and $R \ll 1$, respectively, with $R = \mathcal{R}/\lambda$. In Fig. 3.2 we show the concurrence as a function of $\tau = \lambda t$ in the bad (upper row) and good (lower row) cavity limits. We compare the dynamics of an initially factorized state ($s = 1$) with the one of an initially maximal entangled state ($s = 0$) for four different values of the coupling

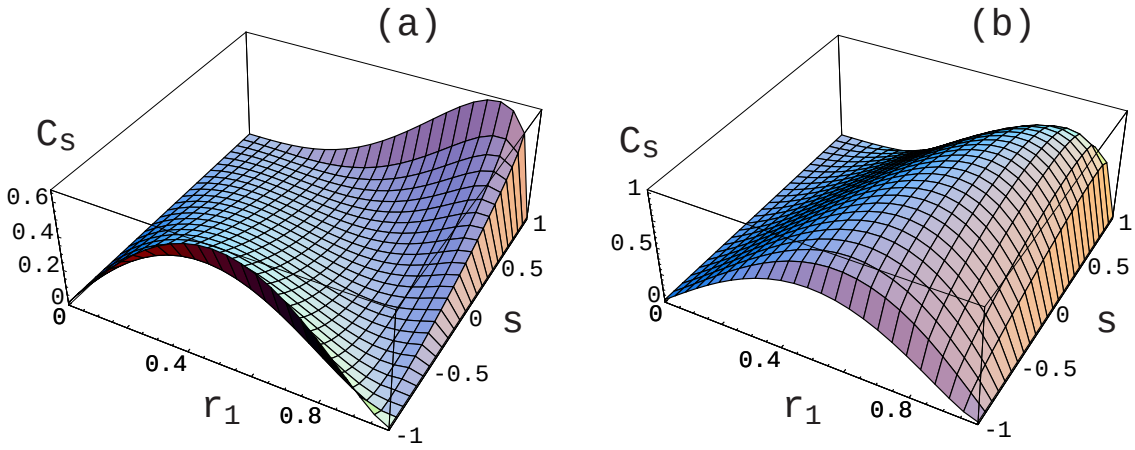

Figure 3.1: (Color online) Stationary concurrence as a function of the relative coupling constant r_1 and of the initial separability s of the state, for (a) $\phi = 0$, and (b) $\phi = \pi$. In the first case, the maximum of C_s is achieved for asymmetrical couplings: at $r_1 \simeq 0.87$ for $s = 1$, and at $r_1 \simeq 0.5$ for $s = -1$. In the second case the maximum is achieved in correspondence of $|\psi(0)\rangle = |\psi_-\rangle$.

parameter r_1, namely $r_1 = 0, 1/\sqrt{2}, 0.87, 1$. The plots for $r_1 = 0$ and $r_1 = 1$ overlap as they both describe a case in which one of the two atoms is effectively decoupled. The value $r_1 = 0.87$ corresponds to the case of optimal stationary entanglement for the initial state $s = 1$ with $\phi = 0$. Finally $r_1 = 1/\sqrt{2}$ corresponds to the case of equal coupling of the two atoms with the reservoir. Other values of r_1 show qualitatively similar behavior.

For weak couplings and/or bad cavity, $R = 0.1$, and for an initially separable state ($s = 1$), the concurrence increases monotonically up to its stationary value; whereas, for initially entangled states, the concurrence first goes to zero before increasing towards C_s. The strong coupling/good cavity case $R = 10$ is more rich and presents entanglement oscillations and revival phenomena for all the initial atomic states. One can prove analytically that for maximally entangled initial states ($s = 0$) the revivals have maximum amplitude when only one of the two atoms is effectively coupled to

the cavity field, i.e. for $r_1 = 0, 1$. In this case, indeed, the system performs damped oscillations between the states $|\psi_+\rangle$ and $|\psi_-\rangle$ which are equally populated at the beginning. On the other hand, for an initially factorized state, the interaction with the cavity field in the strong coupling regime generates a high degree of entanglement. Indeed, for $R = 10$, at $\tau = \bar{\tau} \simeq 0.31$, C attains the value $C(\bar{\tau}) \simeq 0.96$, at $r_1 \simeq 0.92$ (for $s = 1$) or $r_1 \simeq 0.4$ (for $s = -1$).

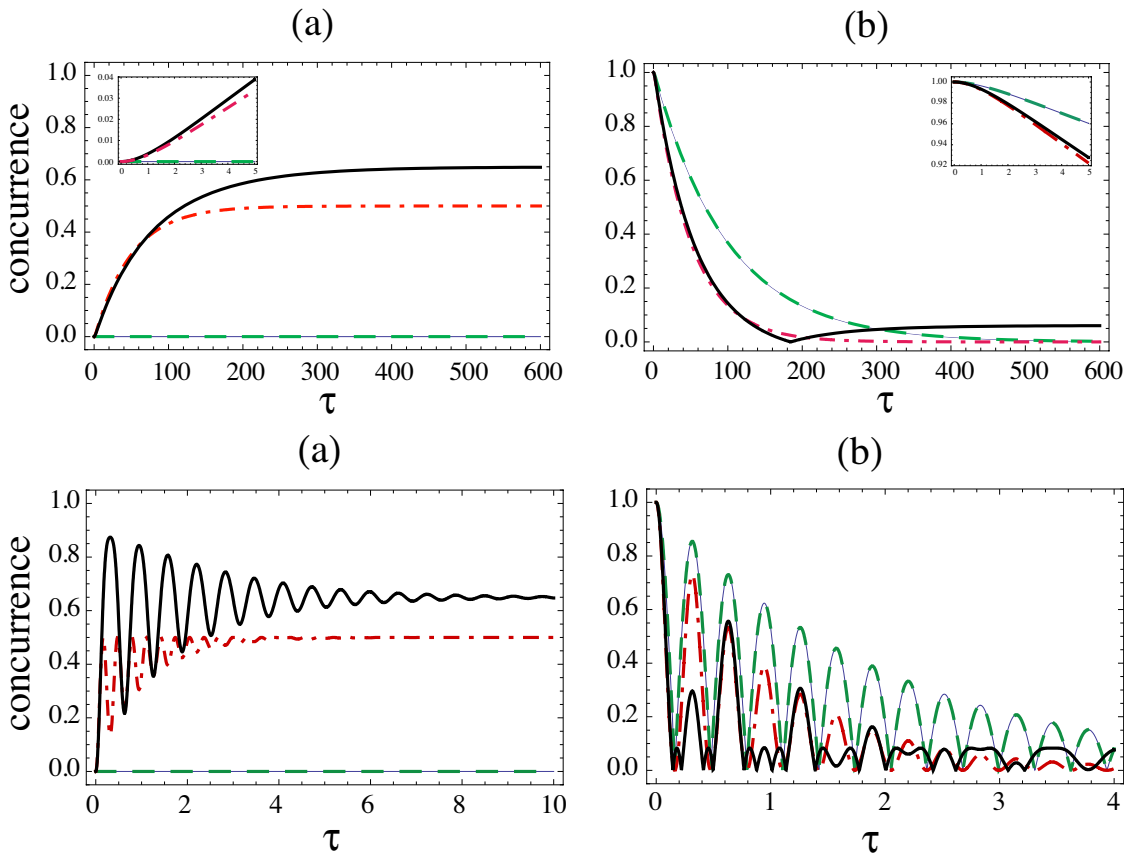

Figure 3.2: (Color online) Time evolution of the concurrence in the bad cavity limit ($R = 0.1$, top plots) and good cavity limit ($R = 10$, bottom plots), with (a) $s = 1$, and (b) $s = 0$, both with $\phi = 0$, for the cases of i) maximal stationary value, $r_1 = 0.87$ (solid line), ii) symmetrical coupling $r_1 = 1/\sqrt{2}$ (dot-dashed line), and iii) only one coupled atom $r_1 = 0, 1$ (dotted line). The insets show the initial quadratic behavior of the concurrence for $R = 0.1$

These entanglement revivals are a truly new result due to the memory depth of the reservoir. Very small revivals can occur in the Markovian regime [**?**], and in the non-Markovian regime with independent reservoirs [67, 91]. In our case, however, the amount of revived entanglement is huge, being comparable to the previous maximum. This feature only appears in the strong coupling regime and with a non-zero environmental correlation time. The surprising aspect, here, is that an irreversible process such as the spontaneous emission is so strongly counteracted by the memory effect of the environment, which not only creates entanglement, but also lets it oscillate quite a few times before a stationary value is reached.

In the next two sections we are going to study how the time evolution of the concurrence is modified in presence of detuning.

3.5 Off-resonant Entanglement in the Subradiant Scenario

We begin considering the case $\omega_1 = \omega_2$. Whenever possible, rather than discussing the exact expression of the concurrence, we will try to derive simpler approximated expressions which are useful for understanding the physical processes taking place in the system.

3.5.1 Bad cavity limit - Enhancement of the entanglement generation

In the bad cavity case, e.g., for $R = \mathcal{R}/\lambda = 0.1$, and for small values of the detuning $\delta < \mathcal{R}$, the behavior of the concurrence does not change appreciably compared to

the resonant case. For values of the detuning $\delta \approx \mathcal{R}$, i.e. when approaching the dispersive regime, the dynamics for an initially factorized state ($s = 1$) shows a monotonic increase towards the stationary value of the concurrence as in the resonant case. However, a significant change occurs in the bad cavity limit when the system is prepared in an initial entangled state. Indeed one can prove that in this regime, contrary to the resonant case, a finite time $\bar{t}$ such that $C(\bar{t}) = 0$ [See Fig. 3.3 (b)] does not exist anymore.

We now focus on the dispersive regime $\delta \gg \lambda \gg \mathcal{R}$. If the qubit-system is initially entangled, e.g., for $s = 0$, the expression for the concurrence can be simplified as follows

$$C(t) = |\mathcal{E}| \approx e^{-\frac{\mathcal{R}^2}{\delta^2}\lambda t}, \qquad \text{for} \quad r_1 = 0, 1; \tag{3.27}$$

$$C(t) = |\mathcal{E}|^2 \approx e^{-2\frac{\mathcal{R}^2}{\delta^2}\lambda t}, \qquad \text{for} \quad r_1 = 1/\sqrt{2}. \tag{3.28}$$

The equations above show that the concurrence vanishes with the decay rate $(\mathcal{R}^2/\delta^2)\lambda$ when only one of the two qubits is coupled to the environment ($r_1 = 0, 1$), and with $2(\mathcal{R}^2/\delta^2)\lambda$ when both qubits are identically coupled to the environment (for $r_1 = 1/\sqrt{2}$). Since $\mathcal{R}/\delta \ll 1$ this proves that in the dispersive regime the decay of entanglement is strongly inhibited compared to the resonant regime since in this case the two atoms exchange energy only via the virtual excitation of the cavity field and therefore the cavity losses do not affect strongly the dynamics.

For large enough detunings the entanglement shows oscillations as a function of time for all of the initial atomic states for which a finite stationary concurrence is obtained, $C_s \neq 0$. Due to the presence of these oscillations and for an initially factorized state, the concurrence reaches values greater than the stationary value C_s even in the bad cavity limit, as shown in Fig. 3.4. For example, for $r_1 = \sqrt{3}/2$,

$R = 0.1$ and $\delta = 10\lambda$, at $\lambda t \approx 2 \times 10^3$ the concurrence reaches the value $C = 0.92$. For an initially factorized state ($s = 1$) and for $r_1 = 1/\sqrt{2}$ we can derive the following approximated expression for the concurrence

$$C(t) \approx \frac{1}{2}\sqrt{1 + e^{-4\frac{\mathcal{R}^2}{\delta^2}\lambda t} - 2e^{-2\frac{\mathcal{R}^2}{\delta^2}\lambda t}\cos\left(2\frac{\mathcal{R}^2}{\delta}t\right)}. \tag{3.29}$$

From this equation one sees that $C(t)$ attains its maximum value at $t = \frac{\pi\delta}{2\mathcal{R}^2}$. This formula also shows that the concurrence undergoes a series of damped oscillations with frequency $2\mathcal{R}^2/\delta$ and decay rate $2(\mathcal{R}/\delta)^2\lambda$.

With increasing detuning, the oscillations become more and more regular, quasi-periodic. The pattern is similar to the oscillations characterizing the strong coupling regime, but now the period is longer. As we will see in Sec. 3.5.2, the generation

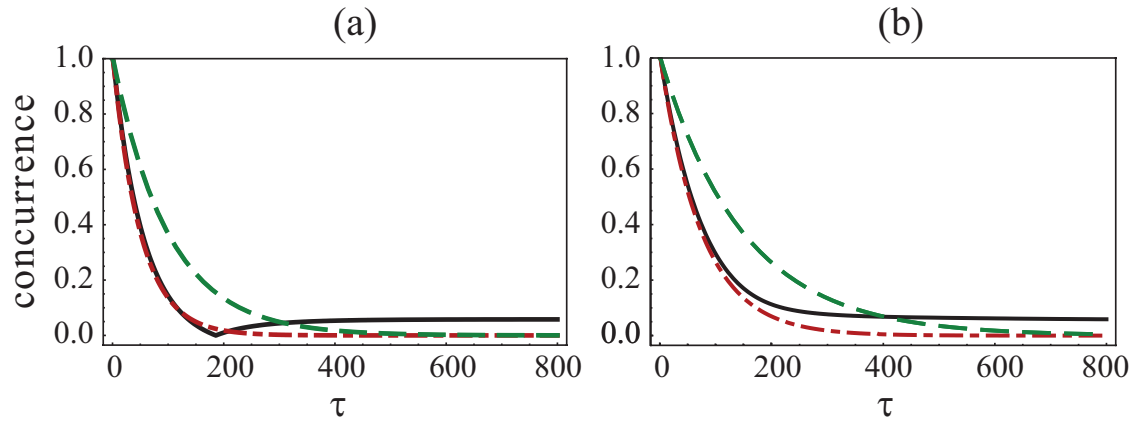

Figure 3.3: (Color online) Time evolution of the concurrence in the bad cavity limit ($R = 0.1$) with $s = 0$ and $\phi = 0$, for the cases of i) maximal stationary value, when $r_1 = \sqrt{3}/2$ (black solid line), ii) symmetrical coupling $r_1 = 1/\sqrt{2}$ (red dot-dashed line), and iii) only one coupled atom $r_1 = 0, 1$ (green dashed line). For each of such cases, we describe the entanglement dynamics in two different coupling regime: the resonant limit (left plot) and for $\delta_1 = \delta_2 = 0.7\lambda$ (right plot).

of a high degree of entanglement in the dispersive regime for initially separable state

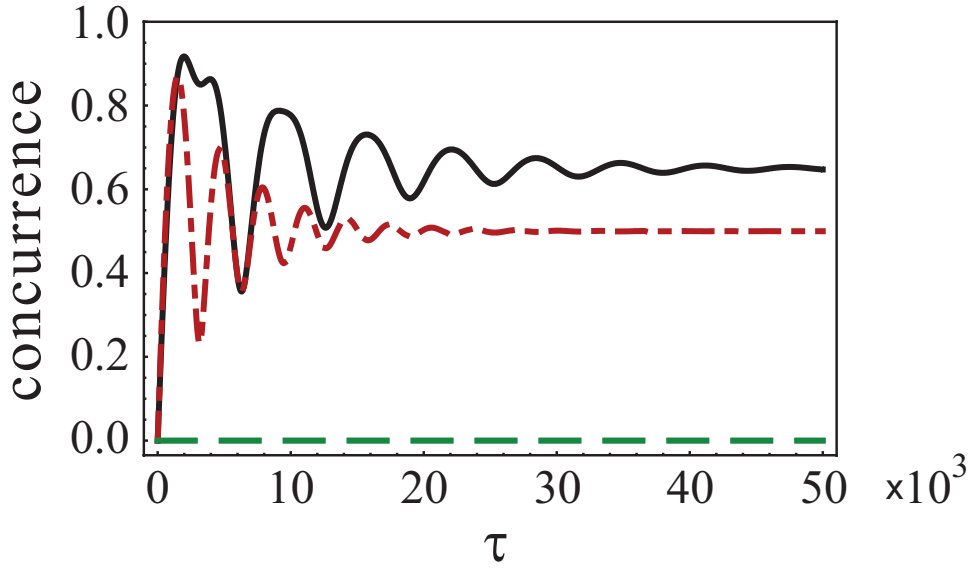

Figure 3.4: (Color online) Time evolution of the concurrence in the bad cavity limit ($R = 0.1$) with $s = 1$, for the cases of i) maximal stationary value, $r_1 = \sqrt{3}/2$ (black solid line), ii) symmetrical coupling $r_1 = 1/\sqrt{2}$ (red dot-dashed line), and iii) only one coupled atom $r_1 = 0, 1$ (green dashed line). All of the plots describe the dispersive regime with $\delta_1 = \delta_2 = 10\lambda$.

can be achieved also in the good cavity limit. However it is remarkable that already in the bad cavity limit, values of concurrence close to one can be generated. Our approach generalizes the results obtained for the dispersive regime in Ref. [88] in the ideal cavity limit to the more realistic case of cavity losses.

3.5.2 Good cavity limit - Entanglement quantum beats

In the strong coupling case entanglement oscillations are present for any initial atomic state. Moreover, for $\delta \approx \lambda \ll \mathcal{R}$, when both atoms are effectively coupled to the cavity field, i.e., $r_1 \neq 0, 1$, the dynamics of concurrence is characterized by the occurrence of quantum beats, as shown in Fig. 3.5. For initially entangled states this phenomenon

is more evident for $\phi = \pi$ because the value of stationary entanglement in this case is higher and the behavior of the concurrence is more regular.

In order to better understand the origin of these entanglement beats, we consider the case $s = 1$ and $r_1 = 1/\sqrt{2}$. For these values of the parameters, and for $\delta \approx \lambda \ll \mathcal{R}$, the expression of the concurrence can be written as follows,

$$C(t) \approx \frac{1}{2}\sqrt{1 + e^{-2\lambda t}\cos(\mathcal{R}t)^4 - 2e^{-\lambda t}\cos(\mathcal{R}t)^2\cos(\delta t)}. \tag{3.30}$$

The term

$$\cos(\mathcal{R}t)^2\cos(\delta t) = \frac{1}{2}\cos(\delta t)\left[1 + \cos(2\mathcal{R}t)\right]$$

in Eq. (3.30), describing an oscillation at frequency $2\mathcal{R}$ modulated by a slower one with frequency δ, is responsible for the occurrence of the quantum beats.

To gain insight in the physical processes characterizing the dynamics, we consider the energy spectrum of the dressed states in the off-resonance case but in the absence of damping, as shown in Fig. 3.6. The diagonalization of the Tavis-Cummings Hamiltonian [See Eq. (B.1) in Appendix B] yields the dressed states

$$|\phi_+\rangle = \frac{1}{\sqrt{\omega_-^2 + \mathcal{R}^2}}\left(-\mathcal{R}|\psi_+\rangle|0\rangle_R + \omega_-|00\rangle|1\rangle_R\right), \tag{3.31}$$

$$|\phi_-\rangle = \frac{1}{\sqrt{\omega_+^2 + \mathcal{R}^2}}\left(-\mathcal{R}|\psi_+\rangle|0\rangle_R + \omega_+|00\rangle|1\rangle_R\right), \tag{3.32}$$

$$|\phi_0\rangle = |\psi_-\rangle|0\rangle_R. \tag{3.33}$$

The corresponding eigenenergies are given by

$$\omega_\pm = \frac{1}{2}\left(\delta \pm \sqrt{4\mathcal{R}^2 + \delta^2}\right), \tag{3.34}$$

$$\omega_0 = \delta, \tag{3.35}$$

where $\mathcal{R} = g\alpha_T$ is the vacuum Rabi frequency and δ is the qubits-cavity detuning.

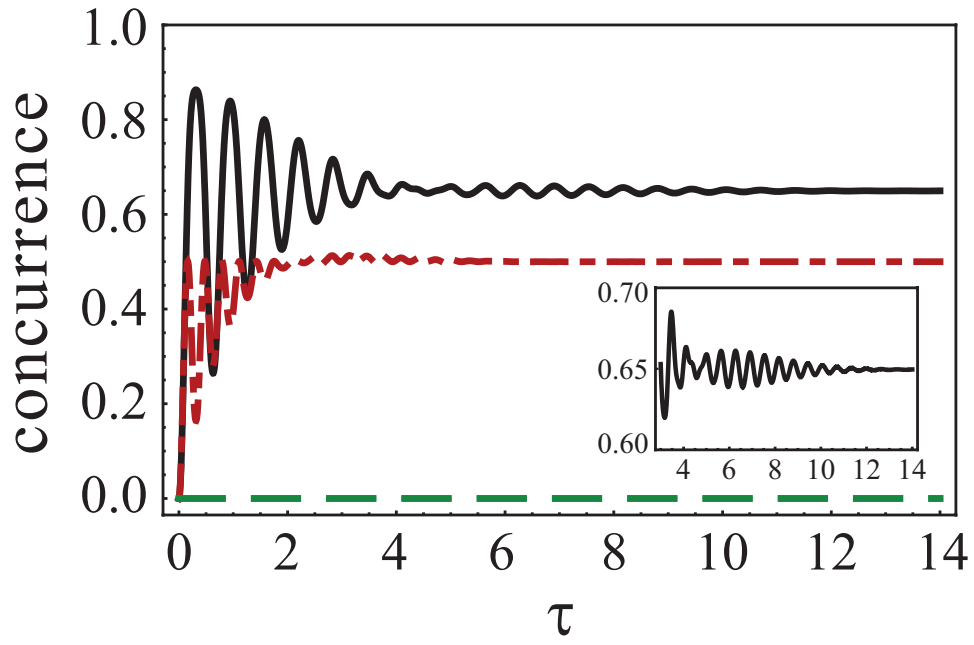

Figure 3.5: (Color online) Time evolution of the concurrence in the good cavity limit ($R = 10$) with $s = 1$, for the cases of i) maximal stationary value $r_1 = \sqrt{3}/2$ (black solid line), ii) symmetrical coupling $r_1 = 1/\sqrt{2}$ (red dot-dashed line), and iii) only one coupled atom $r_1 = 0, 1$ (green dashed line). The curves are drawn for small detuning, $\delta_1 = \delta_2 = 0.7\lambda$; thus, outside the dispersive region. The inset shows the entanglement beat for the case i).

On the other hand, the unperturbed states can be expressed as a superposition of the $|\phi_\pm\rangle$,$|\phi_0\rangle$ eigenstates, with probability amplitudes evolving at frequencies $\omega_\pm$ and ω_0. The effect of the detuning is a shift of the qubits-cavity energy levels, thus the qubits-field coupling gives rise to a reversible energy exchange between unperturbed state at frequencies $2\mathcal{R}$, $\mathcal{R} - \delta/2$ and $\mathcal{R} + \delta/2$. This is clearly seen, e.g., from the

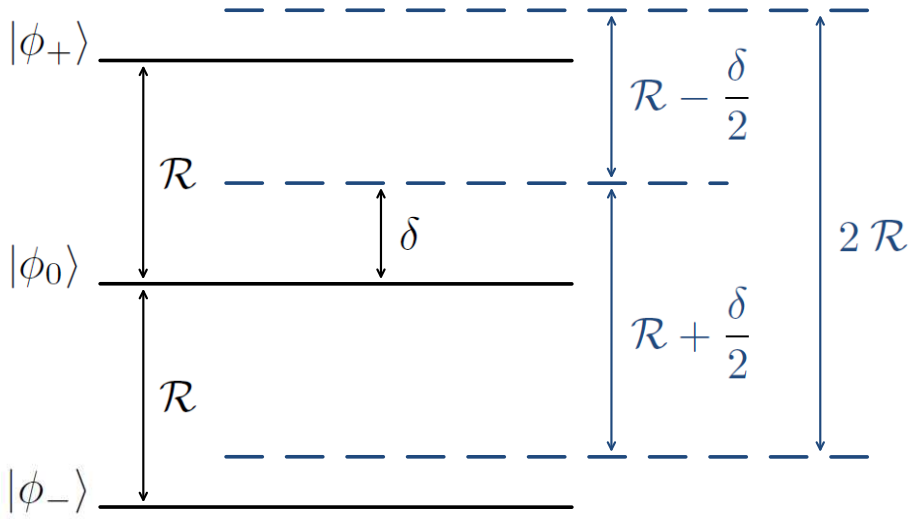

Figure 3.6: (Color online) Energy spectrum of the dressed qubit-photon states in the case of small detuning (blue dashed line) and in the resonant coupling case (black solid line).

time evolution of the populations

$$\begin{aligned} |c_2(t)|^2 &= |\langle 01|\langle 0|e^{-iHt}|01\rangle|0\rangle|^2 \\ &= r_1^4 + \frac{r_2^4}{2}\left[1+\cos(2\mathcal{R}t)\right] + 2r_1^2 r_2^2 \cos\left(\mathcal{R}t\right)\cos\left(\frac{\delta}{2}t\right). \end{aligned}$$

The equation above contains a term oscillating at frequency $2\mathcal{R}$, coming from the coupling between the dressed states $|\phi_+\rangle$ and $|\phi_-\rangle$, and a term oscillating at frequency $\mathcal{R}$ modulated by δ coming from the interference between the oscillations at frequencies $\mathcal{R}-\delta/2$ and $\mathcal{R}+\delta/2$ that couple the states $|\phi_+\rangle$-$|\phi_0\rangle$ and $|\phi_-\rangle$-$|\phi_0\rangle$, respectively.

In the discussion above we have disregarded the cavity losses. When they are taken into account one sees that the dressed energy splitting is resolved, and therefore

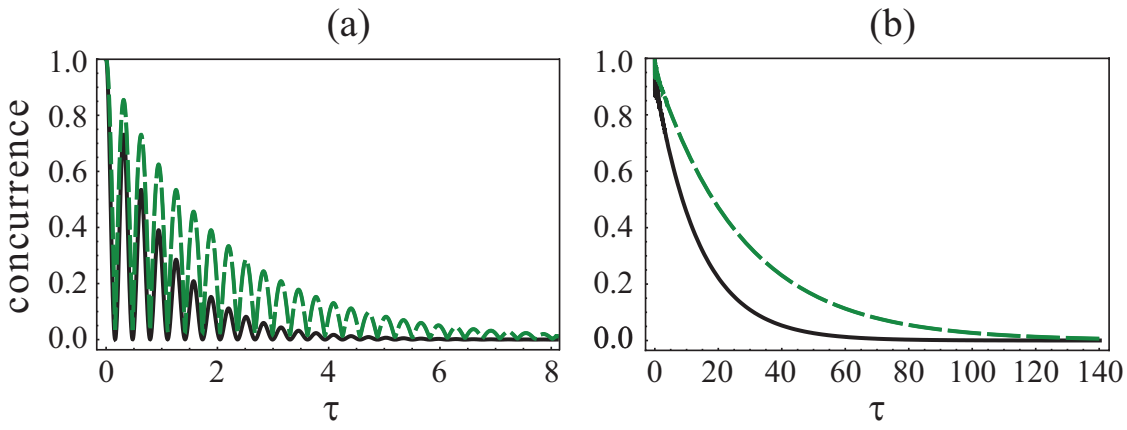

Figure 3.7: (Color online) Time evolution of the concurrence in the good cavity limit ($R = 10$), with $s = 0$ and $\phi = 0$, for the cases of i) symmetrical coupling $r_1 = 1/\sqrt{2}$ (black solid line), and ii) only one coupled atom $r_1 = 0, 1$ (green dashed line). The two plots describe two different detuning regions: $\delta_1 = \delta_2 = 0.7\lambda$ (left) and $\delta_1 = \delta_2 = 50\lambda$ (right).

the quantum beats will be visible, if $2\mathcal{R}$ is larger than the decay width λ. This is achieved in strong coupling regime. Therefore, one does not observe quantum beats in bad cavity case.

We conclude this section studying how the detuning influences the decay of entanglement, for an initially maximally entangled state of the system, and the reservoir-induced entanglement generation, for an initial factorized state.

When only one of the two qubits is effectively coupled to the cavity field, i.e. for $r_1 = 0, 1$, for maximally entangled initial states ($s = 0$) in the resonant regime, $\delta = 0$, the system performs damped oscillations between the states $|\psi_+\rangle$ and $|\psi_-\rangle$, which are equally populated at the beginning. Hence entanglement revivals with maximum amplitude are present in the dynamics, as shown in Fig. 3.7 (a). Increasing the detuning, the amplitude of the oscillations decreases and the revivals disappear, while the frequency does not change appreciably, [See Fig. 3.7 (a)]. In this case the

expression of the concurrence for small values of the detuning can be written as

$$C(t) = |\mathcal{E}| \approx e^{-\lambda t/2}\sqrt{\cos(\mathcal{R}t)^2 + \frac{\delta^2+\lambda^2}{4\mathcal{R}^2}\sin(\mathcal{R}t)^2 - \frac{\lambda}{\mathcal{R}}\sin(\mathcal{R}t)\cos(\mathcal{R}t)}, \qquad (3.36)$$

while for greater values of the detuning, the oscillations completely disappear and the concurrence decays exponentially

$$C(t) = |\mathcal{E}| \approx e^{-\frac{\mathcal{R}^2}{\delta^2}\lambda t}, \qquad (3.37)$$

as shown in Fig. 3.7 (b).

Finally, we note that, similarly to the behavior discussed in the bad cavity limit, when the qubits are initially in a factorized state, the presence of the detuning enhances the generation of entanglement at short times compared to the resonant coupling case, as illustrated in Fig. 3.4. In general, in the strongly dispersive regime, the qubits do not exchange energy with cavity, which is only virtually excited. Thus a high degree of reservoir-induced entanglement can be generated both in the good and in the bad cavity limits.

3.6 Off-resonant Entanglement in the non-subradiant scenario

In this section, we analyze the more general situation in which the transition frequencies of the qubits are different, $\omega_1 \neq \omega_2$, and both qubits are off-resonant with the cavity field. Due to the absence of a subradiant state, even a small value of the detunings $\delta_1, \delta_2 \ll \mathcal{R}$ contributes to accelerate the decay of entanglement for every

initial states. For an initially factorized state, in the bad cavity limit, the entanglement initially created via the interaction with the reservoir is rapidly destroyed as time evolves. In the good cavity limit entanglement oscillations are present and also quantum beats of entanglement can be observed for $\delta_1, \delta_2 \approx \lambda \ll \mathcal{R}$.

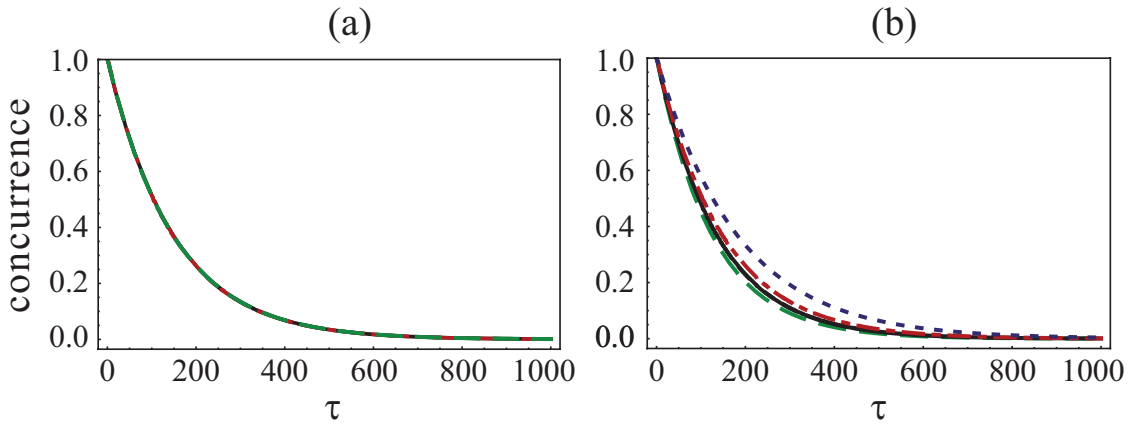

Figure 3.8: (Color online) Time evolution of the concurrence in the bad cavity limit ($R = 0.1$), with $s = 0$ and $\phi = 0$, for the cases of i) maximal stationary value, corresponding to $r_1 = \sqrt{3}/2$ (black solid line), ii) symmetrical coupling $r_1 = 1/\sqrt{2}$ (red dot-dashed line), and iii) only one coupled atom $r_1 = 1$ (green dashed line) and $r_1 = 0$ (blue dotted line). Two different detuning pairs are represented: the symmetrical detuning with $\delta_1 = -0.7\lambda$, $\delta_2 = 0.7\lambda$ (left plot) and the asymmetrical detuning with $\delta_1 = -0.5\lambda$, $\delta_2 = 0.9\lambda$ (right plot).

We now consider in more detail the case in which the two qubits frequencies are symmetrically detuned from the central peak of the Lorentzian spectrum describing the field inside the cavity. In the dispersive region $\delta \gg \mathcal{R}$, and for initially entangled states ($s = 0$), the concurrence vanishes without manifesting a dominant dependence from r_1 and ϕ. In other words, all the states initially entangled decay following the same behavior in such regime, as shown in Fig. 3.8 (a). This is in contrast to what we observed in all other regimes, where a dependence on the value of r_1 is present. We stress once more that this feature seems to occur only for the case of symmetric

detuning. Indeed, when introducing a small asymmetry in the value of the detunings the behavior of the concurrence shows again a dependence on the parameter r_1, as illustrated in Fig. 3.8 (b).

In order to understand the peculiar behavior of the concurrence in the dispersive regime and for symmetric detunings we once more start by neglecting the effect of the cavity losses and use the dispersive Hamiltonian given by Eq. (3.25). For symmetrical detunings $\delta_1 = -\delta_2$ this equation takes the form

$$H_{eff} = -\frac{\mathcal{R}^2 r_1^2}{\delta}\sigma_+^{(1)}\sigma_-^{(1)} + \frac{\mathcal{R}^2 r_2^2}{\delta}\sigma_+^{(2)}\sigma_-^{(2)}, \tag{3.38}$$

with $\delta = |\delta_1| = |\delta_2|$.

Comparing Eq. (3.38) with Eq. (3.25) we notice that the terms describing the effective dipole-dipole coupling induced by the cavity mode are here absent. Therefore the only remaining effect is the entanglement decay induced by the cavity losses. The decay rate, however, does not depend on the relative coupling parameter r_1 but only on the total coupling strength α_T via the vacuum Rabi frequency $\mathcal{R}$. This explains why, even when the cavity losses are taken into account, the time evolution of the concurrence for symmetric detunings does not depend on r_1. When a small asymmetry in the detunings is introduced, the dipole-dipole effective coupling terms are non-zero and, due to the presence of r_1 and r_2 in the effective dipole-dipole coupling strength, the dynamics becomes again dependent on r_1.

3.7 Summary and Conclusions

In this chapter we have provided a complete analysis of the exact dynamics of the entanglement for two qubits interacting with a common zero-temperature reservoir

in the both resonant and off-resonant case. We have presented a general analytical solution for the two-qubit dynamics without performing the Born-Markov approximation. In the case of a Lorentzian spectrum, describing, e.g., the electromagnetic field inside a single mode lossy cavity, we have obtained explicit expressions for the reduced density matrix and for the concurrence. The availability of the exact solution allowed us to look at the entanglement dynamics both in the weak coupling (bad cavity) and in the strong coupling (good cavity) limits.

We analyzed in detail the stationary entanglement and obtained the entanglement dynamics both in the weak and strong coupling limits, showing that entanglement revivals can appear due to the finite memory of such a complex environment.

If the two qubits are initially disentangled, the interaction with the common reservoir generates entanglement. Our results demonstrate that a high degree of entanglement can be generated in this way, especially in the dispersive regime, and even in the bad cavity limit. For initially entangled states, the concurrence decay is slowed down when the qubits are detuned from the peak of the Lorentzian. In this case, indeed, the cavity losses affect less the atoms dynamics since the effective atom-atom interaction is mediated by virtual photon exchange.

In general, the entanglement dynamics is strongly sensitive to the relative coupling parameter r_1, indicating how strongly each of the two qubit is individually coupled to the e.m. field. Only when the qubits frequencies are symmetrically detuned from the main cavity frequency, in the dispersive regime, the dependence on the relative coupling disappears. Finally we have discovered that, in the strong coupling regime, for intermediate values of the detuning, the dynamics of the concurrence shows the

occurrence of quantum beats. We have given a physical interpretation of this phenomenon in terms of the quantum interference between the transitions among the dressed states of the atomic system.

We believe that our results contribute in shedding light on the behavior of quantum entanglement in realistic conditions, that is when the effect of the environment on the quantum system is taken into account. For this reason they have both a fundamental and an applicative value and they indicate how rich the dynamics of this system can be. The model we have studied can be employed to describe both trapped ions in optical cavities and circuit cavity QED dynamics. In both physical contexts, the observation of the effects we have discussed should be achievable with the current experimental technologies. In the first case, it has already been demonstrated that both atoms and ions can be confined inside high finesse optical cavities and their quantum states can be fully controlled [82, 83]. In the second case, quantum communication between two Josephson qubits has been achieved using a transmission line as a cavity [84, 85, 86].

Chapter 4

Quantum Zeno and anti-Zeno effects on the entanglement

4.1 Introduction

The description of decoherence for bipartite entangled systems has recently reached notable theoretical [38, 60] and experimental [37] results due to the introduction of the concept of entanglement sudden death. This describes the finite-time destruction of quantum correlations due to the detrimental action of independent environments coupled to the two subsystems. On the other hand, it is well known [49, 79, 80] that the interaction with a *common* environment leads to the existence of a highly entangled long-living decoherence-free (or sub-radiant) state. At the same time, another entangled state exists (orthogonal to previous one and called super-radiant) that looses its coherence faster.

In this chapter, we discuss how to preserve this second entangled state without affecting the first one by exploiting the quantum Zeno effect in order to achieve a complete entanglement survival.

The effects of very frequent measurements on the decay rate of any unstable

quantum state have been widely discussed in both theoretical [92, 93] and, more recently, experimental works [94, 95]. It was found that frequent measurements can reduce or accelerate the decay process: these are the quantum Zeno and anti-Zeno effects, respectively [96, 97, 98].

Here, we investigate the entanglement dynamics of two qubits coupled to a common reservoir, in presence of measurements. We examine the appearance of quantum Zeno and anti-Zeno effects [99, 96, 97, 98] in the entanglement dynamics of two qubits coupled to the same lossy cavity when the unitary evolution of the system is interrupted by repeated projective measurements. We describe in detail these quantum effects by comparing the measurement-induced coarse-grained dynamics to the entanglement evolution in absence of measurements in several scenarios, as described in the previous chapter. In particular, we examine the strong and weak coupling regimes, the role of the relative coupling strengths between the two qubits and the reservoir, and the effect of the detuning from the main cavity frequency. We show that the anti-Zeno effect can occur in the entanglement dynamics when the qubits frequencies are detuned from the main reservoir frequency. In particular, the quantum Zeno and anti-Zeno effects on entanglement [**?**, 91, 67] stem from the competing action of the off-resonant interaction and of the repeated projective measurements. We find that Zeno and anti-Zeno effects can even appear sequentially many times as a function of the interval between the measurements. Moreover, when the measurement time interval approaches zero, the quantum Zeno effect dominates the dynamics in the far off-resonant limit. Whereas, for greater values of the measurement time interval, the quantum anti-Zeno effect can appear reducing the capability of the system to store entanglement.

Finally we propose a strategy to fight against the deterioration of the entanglement using the quantum Zeno effect. Besides, we show that, in the off-resonant regime, we can preserve the entanglement using the quantum Zeno effect more efficiently than in the resonant limit [**?**], even if, in this case, no sub-radiant state exists.

Furthermore, we describe a measurement induced quantum Zeno effect [99, 98, 100] for the entanglement, showing that the quite simple procedure of monitoring the population of the cavity mode leads to a protection of the entanglement well beyond its natural decay time. This effect too can be tested with slight modifications of already existing experimental set-ups, both in the realm of cavity QED and with superconducting Josephson circuits.

4.2 Observed Entanglement Dynamics

The entanglement dynamics for a generic initial two-qubit state containing one excitation coupled to a common structured reservoir was investigated in the previous chapter. We choose again the concurrence $\mathcal{C}(t)$ [9], ranging from 0 for separable states to 1 for maximally entangled states, to quantify the amount of entanglement encoded into the two-qubit system. The explicit analytic expression of $\mathcal{C}(t)$ can be obtained from the reduced density matrix of Eq. (3.7). It is easy to show that the concurrence takes a very simple form

$$\mathcal{C}(t) = 2\,|c_1(t)|\;|c_2(t)|\,. \tag{4.1}$$

If we express the initial state of the qubits as a superposition of $|\psi_\pm\rangle$, that is $|\psi(0)\rangle = \beta_-|\psi_-\rangle + \beta_+|\psi_+\rangle$, we see that, while part of the initial state will be trapped in the sub-radiant state $|\psi_-\rangle$, another part will decay following Eq. (3.21). Thus, as

discussed above, the amount of entanglement that survives depends on the specific state (and on the value of the r_j). In the following we present a method which exploits the quantum Zeno effect to preserve the initial entanglement *independently* of the state in which it is stored.

Therefore, we analyze the effect of repeated nonselective measurements, performed on the collective qubits system, on the entanglement dynamics in the resonance and in the off-resonance regime. In particular we will demonstrate the occurrence of both quantum Zeno and anti-Zeno effects on the entanglement, depending on the measurement time interval.

We consider the action of a series of nonselective measurements on the collective atomic system, performed at time intervals T, must have the two following properties: i) one of the possible measurement outcomes is the projection onto the collective ground state $|\psi_0\rangle = |0\rangle_1|0\rangle_2$, and ii) the measurement cannot distinguish between the excited-states $|\psi_1\rangle = |1\rangle_1|0\rangle_2$ and $|\psi_2\rangle = |0\rangle_1|1\rangle_2$.

Such measurements are described by the following two projectors:

$$\Pi_0 = |\psi_0\rangle\langle\psi_0| \otimes I_R, \tag{4.2}$$

$$\Pi_1 = (|\psi_-\rangle\langle\psi_-| + |\psi_+\rangle\langle\psi_+|) \otimes I_R, \tag{4.3}$$

with I_R the reservoir identity matrix. The action of the operators above is to project the qubits into the subspace S_1 spanned by

$$|\psi_-\rangle = r_2|1\rangle_1|0\rangle_2 - r_1|0\rangle_1|1\rangle_2,$$

$$|\psi_+\rangle = r_1|1\rangle_1|0\rangle_2 + r_2|0\rangle_1|1\rangle_2.$$

We note that, for $\omega_1 = \omega_2$, the two states above coincide with the subradiant and the superradiant state, respectively. Projective measurements as those described by the

operator Π_0 can be implemented in both cavity QED [82, 83] and in superconducting circuits with on-chip qubits and resonator [85, 86].

Recasting the initial state in the form $|\psi(0)\rangle = \beta_-|\psi_-\rangle + \beta_+|\psi_+\rangle$, we can write the total state at time $t = NT$, i.e., after N measurements of the collective qubits system, as follows

$$\begin{aligned} |\Psi^{(N)}(t)\rangle &= \Pi_1|\Psi^{(N-1)}(t)\rangle \\ &= \left[\beta_-^{(N)}(T)|\psi_-\rangle + \beta_+^{(N)}(T)|\psi_+\rangle\right] \bigotimes_k |0_k\rangle_R. \end{aligned} \tag{4.4}$$

where T is the time interval between two consecutive measurements and $\beta_\pm^{(N)}(T)$ are the survival amplitudes at $t = NT$ in presence of N measurements. The survival amplitudes can be expressed in terms of the initial amplitudes as follows

$$\begin{pmatrix} \beta_+^{(N)}(T) \\ \beta_-^{(N)}(T) \end{pmatrix} = \mathbf{E}^N \begin{pmatrix} \beta_+ \\ \beta_- \end{pmatrix}, \tag{4.5}$$

with

$$\beta_+ = r_1\, c_{10} + r_2\, c_{20}\,, \qquad \beta_- = r_2\, c_{10} - r_1\, c_{20}. \tag{4.6}$$

We characterize the initial state of the qubits in terms of the initial separability s defined via the equations

$$c_{10} = \sqrt{\frac{1-s}{2}}\,, \qquad c_{20} = \sqrt{\frac{1+s}{2}}\, e^{i\,\phi}. \tag{4.7}$$

It is immediate to see that $s = \pm 1$ corresponds to a separable state while $s = 0$ corresponds to a maximally entangled state.

In general, the explicit analytic expressions of the survivor amplitudes $\beta_\pm^{(N)}(T)$ is very complicated and does not provide a simple physical understanding. Nevertheless, one can always calculate the evolution matrix $\mathbf{E}^N$ iteratively.

For $\omega_1 = \omega_2$, a subradiant decoherence-free state $|\psi_-\rangle$ exists. This state does not evolve in time so the only relevant time evolution is the one of the superradiant state $|\psi_+\rangle$. In this case the explicit expression for the survival amplitudes in presence of measurements takes the simple form

$$\beta_-^{(N)}(T) = \beta_- \,, \qquad \beta_+^{(N)}(T) = \mathcal{E}^N(T)\,\beta_+, \tag{4.8}$$

with

$$\mathcal{E}(T) = e^{-(\lambda - i\delta)\,T/2}\left[\cosh\left(\frac{\Omega T}{2}\right) + \frac{\lambda - i\delta}{\Omega}\,\sinh\left(\frac{\Omega T}{2}\right)\right], \tag{4.9}$$

where $\delta_1 = \delta_2 \equiv \delta$ and $\Omega = \sqrt{\lambda^2 - \Omega_R^2 - i2\delta\lambda}$. We indicate with $\Omega_R = \sqrt{4W^2\alpha_T^2 + \delta^2}$ the generalized Rabi frequency and with $\mathcal{R} = W\alpha_T$ the vacuum Rabi frequency. The function $\mathcal{E}(T)$ is the survival amplitude of the superradiant state $\langle\psi_+(T)|\psi_+(0)\rangle = \mathcal{E}(T)$.

The entanglement of the observed two-qubit system, at time $t = NT$, can be evaluate by the concurrence $\mathcal{C}^{(N)}(t)$ in presence of N measurements. This quantity is derived from the reduced density matrix describing the system observed N times, obtained from $|\Psi^{(N)}(t)\rangle\langle\Psi^{(N)}(t)|$ by tracing over the reservoir degrees of freedom. $\mathcal{C}^{(N)}(t)$, in the subradiant scenario ($\omega_1 = \omega_2$), can be written as

$$\begin{aligned}\mathcal{C}^{(N)}(t) \;&=\; 2\Big|\left(r_1\beta_+ e^{i\eta(T)t}e^{-\gamma(T)t/2} + r_2\beta_-\right) \\ &\quad\times\left(r_2\beta_+^* e^{-i\eta(T)t}e^{-\gamma(T)t/2} - r_1\beta_-^*\right)\Big|,\end{aligned} \tag{4.10}$$

where

$$\gamma(T) = -\frac{\log\left[|\mathcal{E}(T)|^2\right]}{T}, \qquad \eta(T) = \frac{\arg\left[\mathcal{E}(T)\right]}{T}, \tag{4.11}$$

are the effective decay rate and the argument of an oscillatory term, respectively.

We note that the dynamics of the concurrence in presence of measurements can be expressed in a simple way in terms of the survival amplitudes $\beta_\pm^{(N)}(T)$ and therefore

depends on T, on the 'position'of the Bohr frequencies of the atoms with respect to the spectrum, on the relative coupling between the qubits and the reservoir, and on the quality factor of the cavity.

In the next section we will see that, for sufficiently short measurement time intervals T, such that $\langle\psi_0|\rho(T)|\psi_0\rangle \ll 1$, both quantum Zeno and anti-Zeno effects on the entanglement may occur.

4.3 Results

In the previous section we have mentioned that the explicit analytical expression for the concurrence $\mathcal{C}^{(N)}(t)$ at time $t = NT$, i.e., after performing N measurements, becomes more complicated in the the off-resonant case. In this section we compare the entanglement dynamics in absence and in presence of measurements for two qubits initially in a maximal entangled state, $(s = 0)$, in both good and bad cavity limits. We not that, in general, the entanglement dynamics in absence of measurements is strongly sensitive to the relative coupling parameter r_1 [101], while we will see that, in presence of measurements, such dependence is often inhibited.

4.3.1 Resonant regime : Protecting entanglement via the quantum Zeno effect

The measurements described above disentangle the qubits from the reservoir at each time T. Choosing T such that $\langle\Psi_g|\rho(T)|\Psi_g\rangle \ll 1$, it is straightforward to prove that the state $|\psi_-\rangle$ is unaffected and that, at the same time, the decay of $|\psi_+\rangle$ is slowed down. Its survival probability $P_+^{(N)}(t) = \langle\psi_+|\rho(t)|\psi_+\rangle$ in presence of N measurements

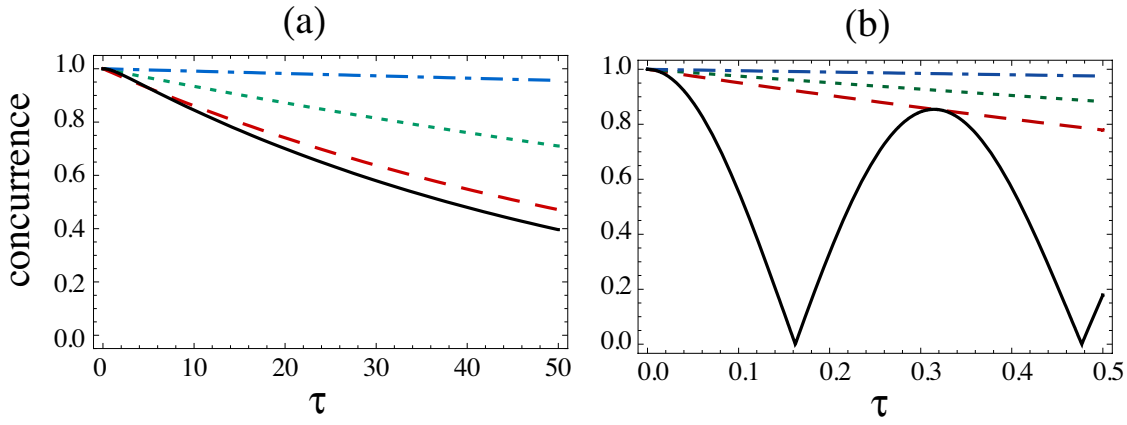

Figure 4.1: Time evolution of the concurrence, for $s = 0$ and $r = 1/\sqrt{2}$, in absence of measurements (solid line) and in presence of measurements performed at intervals (a) $\lambda T = 0.1, 1, 5$ (dashed, dotted and dot-dashed lines, respectively) with $R = 0.1$ (weak coupling) and (b) $\lambda T = 0.001, 0.005, 0.01$ (dashed, dotted, and dot-dashed lines, respectively) with $R = 10$ (strong coupling).

is given by $P_+^{(N)}(t) = |\beta_+(0)|^2 \exp\left[-\gamma_z(T)t\right]$, where $t = NT$ and with an effective decay rate

$$\gamma_z(T) = -\frac{\log\left[\mathcal{E}(T)^2\right]}{T}. \tag{4.12}$$

Notice that, in the limit $T \to 0$ and $N \to \infty$, with a finite $t = NT$, $\gamma_z(T) \to 0$ and the decay is completely suppressed.

Besides affecting the probability $P_+(t)$, the projective measurements also modify the time evolution of the entanglement, whose effective dynamics now depends on T. Explicitly, the concurrence at time $t = NT$, after performing N measurements, is given by

$$C^{(N)}(t) = 2 \left| \left(\beta_+ r_1\, e^{-\gamma_z t/2} + \beta_- r_2\right) \times \left(\beta_+ r_2\, e^{-\gamma_z t/2} - \beta_- r_1\right) \right|. \tag{4.13}$$

In Fig. 4.1 we compare the dynamics of $C(\tau)$ in absence and in presence of measurements performed at various intervals T for an initially maximal entangled state. Both

in the weak and in the strong coupling regimes (left and right plots, respectively) the presence of measurements quenches the decay of the concurrence. Thus, we have achieved a quantum Zeno protection of entanglement from the effect of decoherence. Again, decreasing the interval between the measurements, $C^{(N)}(t)$ remains closer and closer to its initial value.

4.3.2 Bad-cavity limit: Enhancement of the entanglement protection

We begin considering the bad-cavity limit, e.g., $R = \mathcal{R}/\lambda = 0.1$. In the off-resonant case here considered, and at short times, the dynamics of all initially entangled states does not depend strongly on r_1 so we consider the case $r_1 = r_2 = 1/\sqrt{2}$. For small values of the detuning $\delta < \mathcal{R}$ the behavior of the concurrence in presence of measurements does not change appreciably compared to the resonant case. Thus, the observed dynamics shows always the quantum Zeno effect for all values of T. We find a similar result in the dispersive regime, i.e., for values of the detuning $\delta \lesssim \lambda$.

In the subradiant scenario, $\omega_1 = \omega_2$, increasing the detuning the anti-Zeno effect appears for values of T larger than a characteristic threshold value T^* that depends on the detuning, as shown in Fig 4.2. In particular, for increasing values of the detuning, the Zeno region becomes smaller and smaller, occurring only for very short measurements time interval. A similar behavior occurs when only one of the two qubits is coupled to the reservoir, that is $r_1 = 0, 1$.

In the non-subradiant scenario, $\omega_1 \neq \omega_2$, when the detuning is slightly larger than the reservoir width $\delta \gtrsim \lambda$, the dynamics presents new features. In more detail, for $\delta_1 = -\delta_2$, one can prove that the concurrence in presence of measurements shows

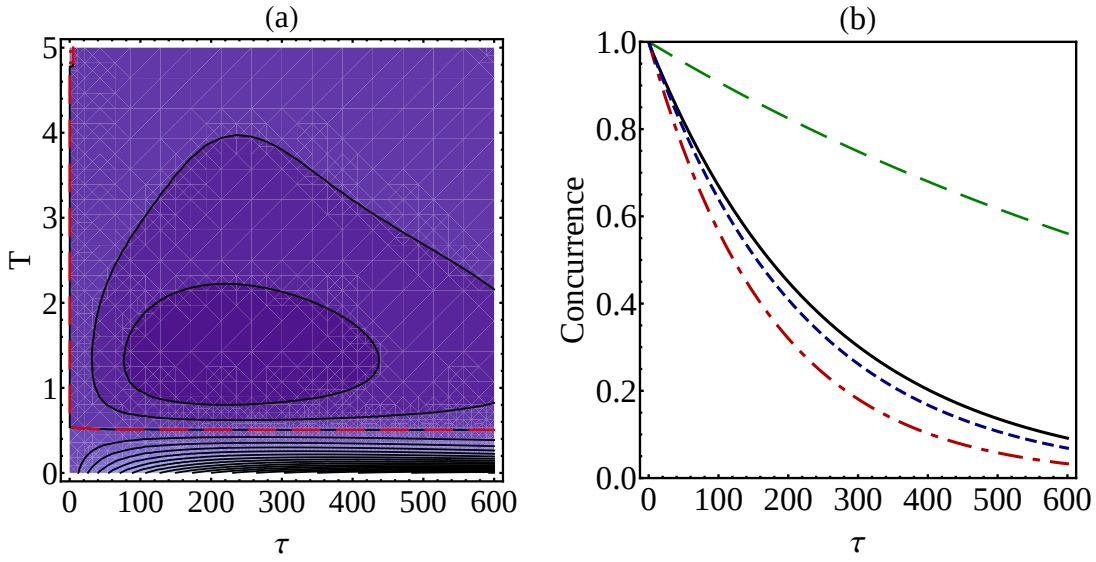

Figure 4.2: (Color online) In the subradiant scenario ($\delta_1 = \delta_2$) and bad cavity limit ($R = 0.1$), for $s = 0$, $\delta = 2$ and $r_1 = 1/\sqrt{2}$: (a) Contour plot of $\mathcal{C}^{(N)}(\tau) - \mathcal{C}(\tau)$ as a function of τ and T (both measured in unit of $1/\lambda$). Large values correspond to lighter shades and the red dashed line is the contour to the value zero. (b) Time evolution of the concurrence in absence of measurements (black solid line) and in presence of measurements performed at time interval: $T = 0.1\lambda$ (green dashed line), $T = 1\lambda$ (red dot-dashed line), $T = 5\lambda$ (blue dotted line).

oscillations as a function of the measurements time interval T, thus quantum Zeno and anti-Zeno effects for the entanglement alternatively occur for increasing values of T, as shown in Fig 4.3. Moreover, for $\delta \sim \lambda$, the quantum Zeno effect dominates again the dynamics for time intervals T of the order of the reservoir memory time. In this regime an interesting phenomenon happens namely the quantum Zeno protection of entanglement is more efficient than in the resonant case, also for longer times.

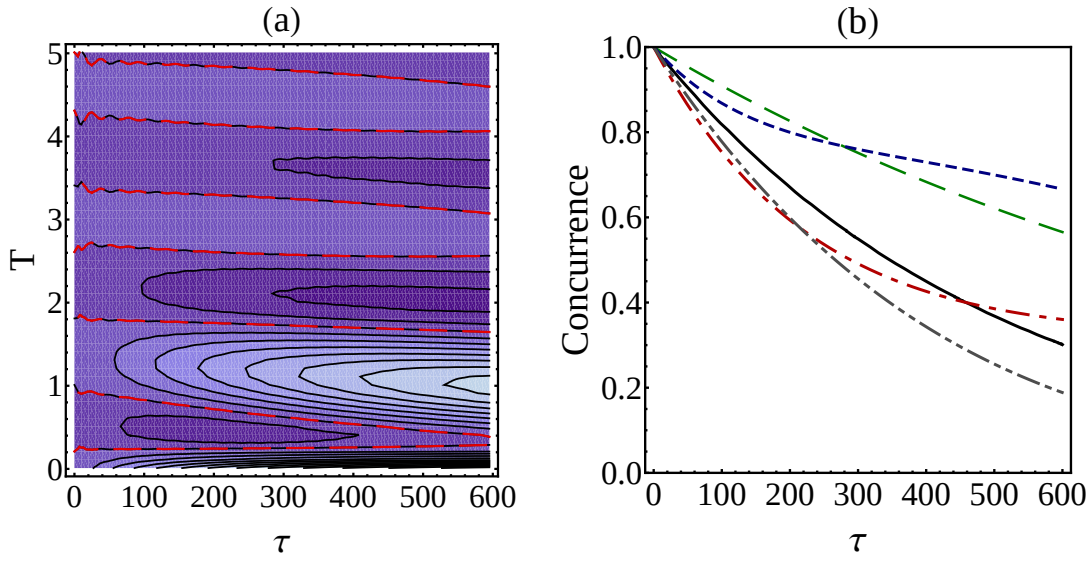

Figure 4.3: (Color online)In the non-subradiant scenario ($\delta_1 = -\delta_2$) and bad cavity limit ($R = 0.1$), for $s = 0$, $\delta = 2$ and $r_1 = 1/\sqrt{2}$: (a) Contour plot of $\mathcal{C}^{(N)}(\tau) - \mathcal{C}(\tau)$ as a function of τ and T (both measured in units of $1/\lambda$). Larger values correspond to lighter shades and the red dashed line is the contour to the value zero. (b) Time evolution of the concurrence in absence of measurements (black solid line) and in presence of measurements performed at time interval: $T = 0.1\lambda$ (green dashed line), $T = 0.5\lambda$ (red dot-dashed line), $T = 1\lambda$ (blue dotted line), $T = 2\lambda$ (gray dot-dot-dashed line).

4.3.3 Good-cavity limit: Monotone entanglement dynamics

In the good cavity limit, e.g., for $R = \mathcal{R}/\lambda = 10$, the behavior of the concurrence in absence of measurements shows entanglement oscillations and revival phenomena due to the non-Markovian memory of the reservoir. Projective measurements performed on the qubits at time intervals T shorter than the reservoir memory time disentangle the qubits from the reservoir and destroy the entanglement oscillations and revival phenomena due to the system-reservoir correlations. In other words, the measurements suppress more and more efficiently the feedback from the reservoir into the

qubits the shorter is T.

Thus, unlike the bad cavity case, in this regime the entanglement dynamics in presence of measurements shows qualitatively similar behaviors for all values of the detuning as well as for both $r_1 = r_2 = 1/\sqrt{2}$ and $r_1 \neq r_2$. However, the Zeno and anti-Zeno regions still depend on r_j because the concurrence in absence of measurements is strongly sensitive to the relative coupling parameter.

For values of the detuning $\delta < \mathcal{R}$, the system presents quantum Zeno effect for all values of T, independently of the relative coupling r_j. In the dispersive regime $\delta > \mathcal{R}$, when both qubits are identically coupled to the reservoir $\left(r_1 = 1/\sqrt{2}\right)$, the concurrence in presence of measurements decreases monotonically to zero and the anti-Zeno effect occurs for values of T greater than a characteristic threshold value T^* that depends on the detuning, as shown in Fig 4.4. For increasing values of the detuning the entanglement dynamics in presence of measurements does not change appreciably: the amplitude of the oscillations decreases until it reaches the value obtained in absence of measurements and the value of T^* decreases.

For $r_1 \neq 1/\sqrt{2}$, the entanglement dynamics in presence of measurements start to decrease approaching zero and then increases again towards its stationary value, which is zero only in the non-subradiant scenario. Although, the concurrence shows always a qualitatively similar behavior, the Zeno and anti-Zeno regions depend on the different detuning configurations, as one can understand by looking at the concurrence behavior in absence of measurements, see Fig 4.5. Finally, we note that, in the good cavity limit the presence of the detuning enhances the appearance of the quantum anti-Zeno effect on the entanglement.

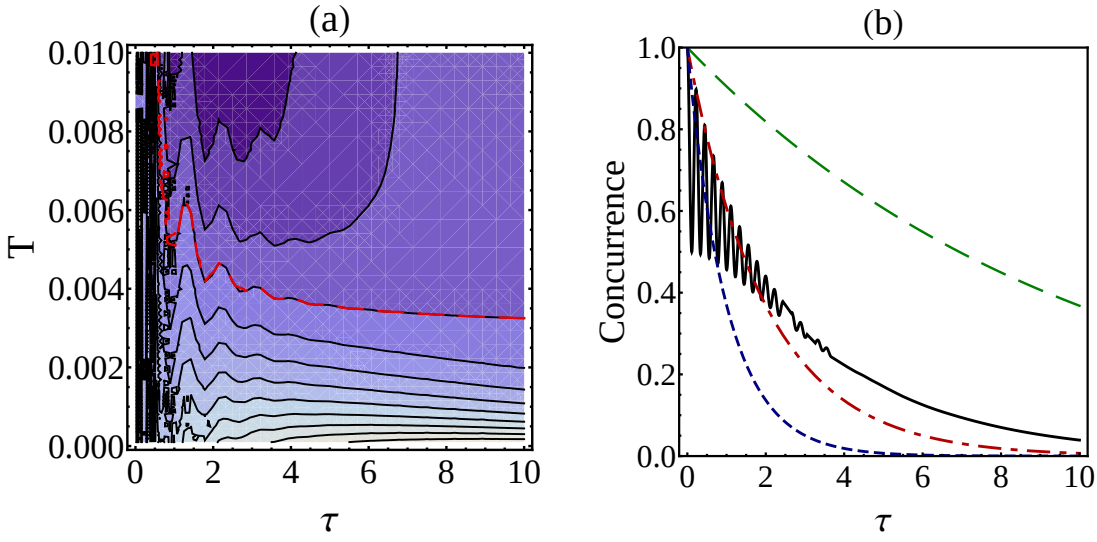

Figure 4.4: (Color online) In the subradiant scenario ($\delta_1 = \delta_2$) and good cavity limit ($R = 10$), for $s = 0$, $\delta = 20$ and $r_1 = 1/\sqrt{2}$: (a) Contour plot of $\mathcal{C}^{(N)}(\tau) - \mathcal{C}(\tau)$ as a function of τ and T (both measured in unit of $1/\lambda$), where larger values are shown lighter and the red dashed line is the contour to the value zero. (b) Time evolution of the concurrence in the absence of measurements (black solid line) and in the presence of measurements performed at time interval: $T = 0.001\lambda$ (green dashed line), $T = 0.005\lambda$ (red dot-dashed line), $T = 0.01\lambda$ (blue dotted line).

4.4 Summary and Conclusions

In this chapter we investigated the entanglement dynamics in presence of measurements and looked at the conditions for the occurrence of both the quantum Zeno and the anti-Zeno effects on the entanglement.

We investigated the quantum Zeno effect for this system, showing that the entanglement can be preserved independently of the state in which it is encoded, with the help of repeated projective measurements.

We found that the quantum Zeno effect always occurs when the measurements

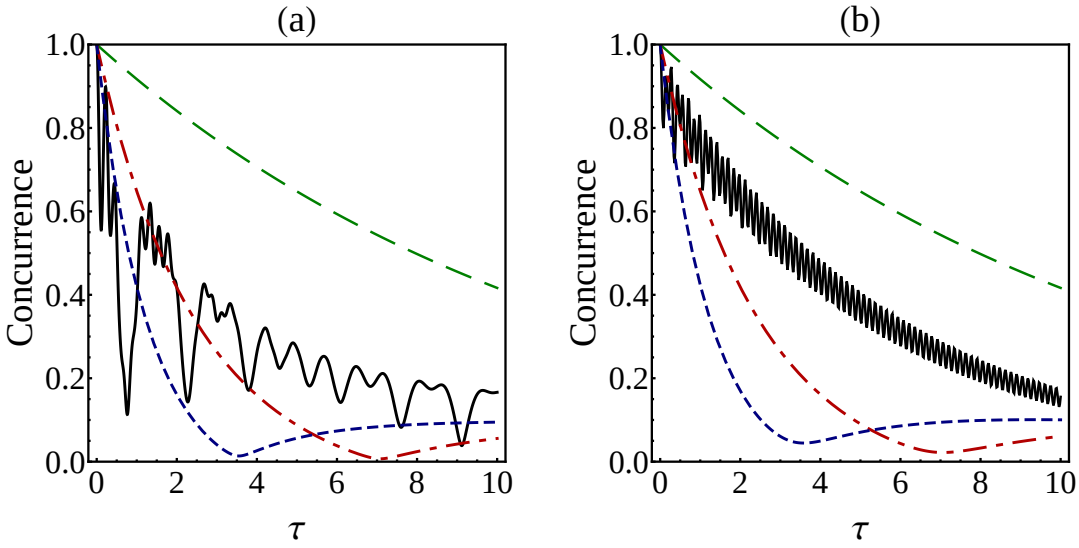

Figure 4.5: (Color online) Time evolution of the concurrence in the good cavity limit ($R = 10$), for $s = 0$, $\delta = 20$ for $r_1 = 0.4$ in absence of measurements (black solid line) and in presence of measurements performed at time interval: $T = 0.001\lambda$ (green dashed line), $T = 0.005\lambda$ (red dot-dashed line), $T = 0.01\lambda$ (blue dotted line). The two plots describe two different detuning configurations: (a) $\delta_1 = \delta_2 = 20\lambda$ and (b) $-\delta_1 = \delta_2 = 20\lambda$.

time interval T approaches zero, while for larger values of T, also the quantum anti-Zeno effect may occur. For certain values of the parameters, increasing values of T correspond to an alternative appearance of the Zeno and anti-Zeno effects .

In the bad cavity limit both the behavior of the concurrence in presence of measurements and the Zeno and anti-Zeno regions are essentially independent of r_j. Finally, we note that, when the measurement time interval is of the order of the reservoir memory time, the presence of the detuning enhances the protection of entanglement compared to the resonant case, so the entanglement can be more effectively protected for long times. On the contrary, in the good cavity limit the presence of the detuning enhances the appearance of the quantum anti-Zeno effect on the entanglement.

Appendix A

Analytic solution for the probability amplitudes

In this Appendix we briefly discuss the structure of the analytical solutions of Eqs. (3.14)-(3.15) for the probability amplitudes $c_{1,2}(t)$ and how they can be obtained applying the Laplace transform method. We note that the solutions obtained in this way are exact since we do not perform any kind of approximation.

The solution of the Laplace transformed amplitudes $\widetilde{c}_{1,2}(s)$, obtained from Eqs. (3.16)-(3.17) can be written as the sum of three ratios having denominators $(s - s_i)$, where s_i are the roots of the cubic equation.

$$s^3 + A_j s^2 + B_j s + C_j = 0, \qquad (j = 1, 2) \tag{A.1}$$

where

$$\begin{aligned} A_{1,2} &= \lambda + i\,(\delta_{2,1} - 2\,\delta_{1,2})\,, \\ B_{1,2} &= \mathcal{R}^2 - \delta_{1,2}^2 + \delta_1\,\delta_2 + i\,(\delta_{2,1} - \delta_{1,2})\,\lambda, \\ C_{1,2} &= i\,\mathcal{R}^2\,r_{1,2}^2\,(\delta_{2,1} - \delta_{1,2})\,. \end{aligned}$$

The amplitudes $c_{1,2}(t)$, obtained by inverse Laplace transform will then be the sum of three damped oscillating terms having, in general, a complicated structure. Only for the case $\omega_1 = \omega_2$ a simple analytical expressions for the probability amplitudes can be obtained, whereas in the general case there is no simple solution. This is because, when $\omega_1 = \omega_2$ the cubic equation can be written as a product of polynomials of first and second order having always one root coincident with zero. In this case one can write the amplitudes in the simple form given by Eqs. (3.19)-(3.20).

Appendix B

Effective dispersive Hamiltonian

The Hamiltonian describing the interaction between two-qubit systems and the quantized cavity mode is given by

$$\begin{aligned} H &= \sum_{j=1}^{2} \omega_j \sigma_+^{(j)} \sigma_-^{(j)} + \omega_c b^\dagger b \\ &\quad + \left[g \left(\alpha_1 \sigma_+^{(1)} + \alpha_2 \sigma_+^{(2)} \right) b + \text{h.c.} \right]. \end{aligned}$$

To obtain the effective Hamiltonian describing the interaction with the cavity in the dispersive regime, one can apply the canonical transformation defined by the unitary operator [89, 90]

$$e^{\alpha S} = e^{-\sum_{j=1}^{2} \frac{\mathcal{R}r_j}{\delta_j} \left(b \sigma_+^{(j)} - b^\dagger \sigma_-^{(j)} \right)} \tag{B.1}$$

with $\mathcal{R}r_j = g\alpha_j$. This procedure is correct to the second order in the coupling to the cavity, and, limiting ourselves to this approximation, we can write the effective Hamiltonian as follows

$$H_{eff} = e^{\alpha S} H e^{-\alpha S} \simeq H + \alpha[S, H] + \frac{\alpha^2}{2}[S, [S, H]].$$

Assuming that the cavity field is initially in the vacuum state, H_{eff} takes the form

$$H_{eff} = \sum_{j=1}^{2} \frac{\mathcal{R}^2\, r_j^2}{\delta_j}\, \sigma_+^{(j)}\sigma_-^{(j)} + \frac{\mathcal{R}^2\, r_1 r_2}{2\,\delta_j} \left(\sigma_+^{(1)}\sigma_-^{(2)} + \sigma_+^{(2)}\sigma_-^{(1)}\right), \tag{B.2}$$

where the terms proportional to $\sigma_+^{(j)}\sigma_-^{(j)}$ describe the Stark shifts due to the dispersive interaction, while the last two terms describe the dipole-dipole coupling between the two atoms induced by the cavity mode through the exchange of virtual cavity photons.

Appendix C

Approximate expressions of the concurrence

In this Appendix we derive approximate expressions for the amplitudes $c_{1,2}(t)$ in the case of large (and equal) detuning $\delta \gg \lambda \gg \mathcal{R}$.

For this purpose, we expand the term $\Omega = \sqrt{\lambda^2 - \Omega_R^2 - i2\delta\lambda}$ as follows,

$$\Omega \approx \lambda \left(1 - \frac{2\,\mathcal{R}^2}{\delta^2}\right) - i\left(\delta + \frac{2\,\mathcal{R}^2}{\delta}\right). \tag{C.1}$$

The temporal evolution described by $\mathcal{E}(t)$ can then be written as

$$\begin{aligned} \mathcal{E}(t) &\approx e^{-(\lambda - i\delta)t/2}\left[\cosh\left(\frac{\Omega t}{2}\right) + \sinh\left(\frac{\Omega t}{2}\right)\right] \\ &\approx e^{-\frac{\mathcal{R}^2}{\delta^2}(\lambda + i\delta)t}. \end{aligned}$$

For the sake of simplicity we consider here the case $s = 1$ and $r_1 = 1/\sqrt{2}$. However the time evolution of the concurrence has features in common with all of the other

cases:

$$\begin{aligned} C(t) &= 2\,|c_1(t)|\,|c_2(t)| \\ &= \frac{1}{2}\sqrt{(1+|\mathcal{E}(t)|^2)^2-(2\,Re[\mathcal{E}(t)])^2} \\ &\approx \frac{1}{2}\sqrt{1+e^{-4\frac{\mathcal{R}^2}{\delta^2}\lambda t}-2e^{-2\frac{\mathcal{R}^2}{\delta^2}\lambda t}\cos\left(2\frac{\mathcal{R}^2}{\delta}t\right)}. \end{aligned}$$

On other hand, for small detunings of the order of λ, outside the dispersive region $\delta \ll \mathcal{R}$, the approximate form of Ω is given by

$$\Omega \approx \frac{\lambda\,\delta}{2\,\mathcal{R}} - i2\,\mathcal{R}, \tag{C.2}$$

so that the time evolution is described by the function

$$\begin{aligned} \mathcal{E}(t) &\approx e^{-(\lambda-i\delta)t/2}\left[\cosh\left(\frac{\Omega t}{2}\right)-\frac{\delta+i\lambda}{2\,\mathcal{R}}\sinh\left(\frac{\Omega t}{2}\right)\right] \\ &\approx e^{-(\lambda-i\delta)t/2}\left[\cos\left(\mathcal{R}t\right)-\frac{\lambda}{2\,\mathcal{R}}\sin\left(\mathcal{R}t\right)+i\frac{\delta}{2\,\mathcal{R}}\sin\left(\mathcal{R}t\right)\right]. \end{aligned}$$

Therefore, for the case $s=1$ and $r_1=1/\sqrt{2}$ the time evolution of the concurrence is given by

$$\begin{aligned} C(t) &= \frac{1}{2}\sqrt{(1+|\mathcal{E}(t)|^2)^2-(2\,Re[\mathcal{E}(t)])^2} \\ &\approx \frac{1}{2}\sqrt{1+e^{-2\lambda t}\cos(\mathcal{R}t)^4-2e^{-\lambda t}\cos(\mathcal{R}t)^2\cos(\delta t)}. \end{aligned}$$

Bibliography

[1] N. Rosen A. Einstein, B. Podolsky. Can quantum-mechanical description of physical reality be considered complete? *Phys. Rev.*, 47:777, 1935.

[2] J. S. Bell. On the einstein-podolsky-rosen paradox. *Physics (Long Island City, N.Y.)*, 1:195, 1964. Reprinted in J.S.Bell: *Speakable and unspeakable in quantum mechanics*, Cambridge University Press, 1987.

[3] J.Smolin W.K.Wootters C.H.Bennet, D.P.DiVincenzo. Mixed-state entanglement and quantum error correction. *Phys. Rev. A*, 54:3824, 1996.

[4] M. Rippin V. Vedral, M. Plenio and P. Knight. Quantifying entanglement. *Phys. Rev. Lett.*, 78(12):2275–2279, 1997.

[5] V. Vedral and M. Plenio. Entanglement measures and purification procedures. *Phys. Rev. A*, 57(3):1619–1633, 1998.

[6] G.Vidal. Entanglement monotones. *J. Mod. Opt.*, 47:355, 2000.

[7] S.Popescu B.Schumacher C.H.Bennet, H.J.Bernstein. Concentrating partial entanglement by local operations. *Phys. Rev. A*, 53:2046, 1996.

[8] D.Bohm. A suggested interpretation of the quantum theory in terms of "hidden" variables. i. *Phys. Rev.*, 85(166), 1952.

[9] W.K. Wootters. *Phys. Rev. Lett.*, 80:2245, 1998.

[10] S.Popescu B.Schumacher J.A.Smolin W.K.Wootters C.H.Bennett, G.Brassard. Purification of noisy entanglement and faithful teleportation via noisy channels. *Phys. Rev. Lett.*, 76:722–725, 1996.

[11] A.Uhlmann. Fidelity and concurrence of conjugated states. *Phys. Rev. A*, 62:032307, 2000.

[12] A.Uhlmann. Entropy and optimal decompositions of states relative to a maximal commutative subalgebra. *quant-ph/9704017*, 1998.

[13] M.Horodecki. Entanglement measures. *Quantum Inf. Comput. 1*, 2001.

[14] R.F.Werner K.G.H.Vollbrecht. Entanglement measures under symmetry. *Phys. Rev. A*, 64:062307/1–15, 2001.

[15] K.G.H.Vollbrecht B.M.Terhal. Entanglement of formation for isotropic states. *Phys. Rev. Lett.*, 85:2625, 2000.

[16] W.K.Wootters S.Hill. Entanglement of a pair of quantum bits. *Phys. Rev. Lett.*, 78:5022–5025, 1997.

[17] W.K.Wootters. Entanglement of formation and concurrence. *Quantum Information and Computation*, 1(1):27–44, 2001.

[18] H.D. Zeh. On the interpretation of measurement in quantum theory. *Found. Phys.*, 1:69–76, 1970.

[19] C.W. Gardiner. *Quantum Noise.* Springer, Berlin, 1991.

[20] W.H. Zurek. *Phys. Today*, 44:1036, 1991.

[21] E. Schrödinger. *Die Naturwiss*, 23:807, 1935.

[22] A. O. Caldeira and A. J. Leggett. *Phys. Rev. Lett.*, 46:211, 1981.

[23] A. O. Caldeira and A. J. Leggett. *Ann. of Phys. (New York)*, 149:374, 1983.

[24] A. T. Dorsey M. P. A. Fisher A. Garg A. J. Leggett, S. Chakravarty and W. Zwerger. *Rev. Mod. Phys.*, 59:1, 1987.

[25] H. Grabert U. Weiss and S. Linkwitz. *J. Low Temp. Phys.*, 68:213, 1987.

[26] H.D. Zeh. Toward a quantum theory of observation. *Found. Phys.*, 3:109–116, 1973.

[27] H.D. Zeh O. Kübler. Dynamics of quantum correlations. *Ann. Phys. (N.Y.)*, 76:405–418, 1973.

[28] H.D. Zeh E. Joos. The emergence of classical properties through interaction with the environment. *Z. Phys. B: Condens. Matter*, 59:223–243, 1985.

[29] W.H. Zurek. Pointer basis of quantum apparatus: Into what mixture does the wave packet collapse? *Phys. Rev. D*, 24:1516–1525, 1981.

[30] W.H. Zurek. Environment-induced superselection rules. *Phys. Rev. D*, 26:1862–1880, 1982.

[31] W.H. Zurek. Reduction of the wavepacket: How long does it take? *Frontiers of Nonequilibrium Statistical Mechanics*, pages 1145–149, 1986.

[32] V. Patel W. Chen S. K. Yolpygo Friedman, J. R. and J. E. Lukens. *Nature*, 43, 2000.

[33] A. C. J. ter Haar F. K. Wilhelm R. N. Schouten C. J. P. M. Harmans T. P. Orlando S. Lloyd van der Wal, C. H. and J. E. Mooij. *Science*, 290:773, 2000.

[34] M. A. Nielsen and I. L. Chuang. *Quantum Computation and Quantum Information*. Cambridge, England, 2000.

[35] J. M. Raimond L. Davidovich, M. Brune and S. Haroche. *Phys. Rev. A*, 53:1295, 1996.

[36] J. Dreyer X. Maître A. Maali C. Wunderlich J. M. Raimond M. Brune, E. Hagley and S. Haroche. *Phys. Rev. Lett.*, 77:4887, 1996.

[37] M.P. Almeida et al. *Science*, 316:579, 2007.

[38] T. Yu and J.H. Eberly. *Phys. Rev. Lett.*, 93:140404, 2004.

[39] T. Yu and J.H. Eberly. *Science*, 323:598, 2009.

[40] T. Yu and J.H. Eberly. *Opt. Comm.*, 264:393, 2006.

[41] T. Yu and J.H. Eberly. *Phys. Rev. B*, 66:193306, 2002.

[42] J. von Neumann. *Mathematical Foundations of Quantum Mechanics*. Princeton University Press, Princeton, NJ, 1955.

[43] A. O. Caldeira and A. J. Leggett. *Physica A*, 121:587, 1983.

[44] Y. Zhang B.L. Hu, J.P. Paz. *Phys. Rev. D*, 45:2843, 1992.

[45] C. Kiefer D. Giulini J. Kupsch I.-O. Stamatescu E. Joos, H. D. Zeh. *Decoherence and the Appearance of a Classical World in Quantum Theory*. Springer, New York, 2003.

[46] W. G. Unruh and W. H. Zurek. *Phys. Rev. D*, 40:1071, 1989.

[47] W.H. Zurek. Decoherence, einselection, and the quantum origins of the classical. *Rev. Mod. Phys.*, pages 715–775, 2003.

[48] S. Habib W.H. Zurek and J. P. Paz. Coherent states via decoherence. *Phys. Rev. Lett.*, 70:1187, 1993.

[49] A. K. Ekert G. M. Palma, K.-A. Suominen. Quantum computers and dissipation. *Proc. R. Soc. Lond. A*, 452:567–584, 1996.

[50] K. B. Whaley D. A. Lidar, I. L. Chuang. Decoherence-free subspaces for quantum computation. *Phys. Rev. Lett.*, 81:2594–2597, 1998.

[51] M. Rasetti P. Zanardi. Noiseless quantum codes. *Phys. Rev. Lett.*, 79:3306–3309, 1997.

[52] G.-C. Guo L.-M. Duan. Reducing decoherence in quantum-computer memory with all quantum bits coupling to the same environment. *Phys. Rev. A*, 57:737–741, 1998.

[53] W.H. Zurek. Preferred states, predictabilty, classicality, and the environmentinduced decoherence. *Prog. Theor. Phys.*, 89:281–312, 1993.

[54] W.H. Zurek. Decoherence, einselection, and the existential interpretation. *Philos. Trans. R. Soc. London, Ser. A*, 356:1793–1821, 1998.

[55] L. Davidovich M. F. Santos, P. Milman and N. Zagury. Direct measurement of finite-time disentanglement induced by a reservoir. *Phys. Rev. A*, 73:040305, 2006.

[56] J. Podany A. F. Starace J. Wang, H. Batelaan. *J. Phys. B*, 39:4343, 2006.

[57] J. S. Pratt. *Phys. Rev. Lett.*, 93:237205, 2004.

[58] P. L. Knight S. Bose, I. Fuentes-Guridi and V. Vedral. *Phys. Rev. Lett.*, 87:050401, 2001.

[59] R. Werner. Quantum states with einstein-podolsky-rosen correlations admitting a hidden-variable model. *Phys. Rev. A*, 40:4277, 1989.

[60] T. Yu and J.H. Eberly. *Phys. Rev. Lett.*, 97:140403, 2006.

[61] J. Laurat et al. *Phys. Rev. Lett.*, 99:180504, 2007.

[62] Z. Ficek and R. Tanaś. *Phys. Rev. A*, 77:054301, 2006.

[63] F. Lastra E. Solano C. E. Lopez, G. Romero and J. C. Retamal. *Phys. Rev. Lett.*, 101:080503, 2008.

[64] J. H. Eberly and T. Yu. *Science*, 316:555, 2007.

[65] J. Lee P. Marek and M. S. Kim. *Phys. Rev. A*, 77:032302, 2008.

[66] A. Al-Qasimi and D. F. V. James. *Phys. Rev. A*, 77:012117, 2008.

[67] R. Lo Franco B. Bellomo and G. Compagno. *Phys. Rev. Lett.*, 99:160502, 2007.

[68] R. Lo Franco B. Bellomo and G. Compagno. *Phys. Rev. A*, 77:032342, 2008.

[69] I. Sainz and G. Bjöörk. *Phys. Rev. A*, 76:042313, 2007.

[70] R. Floreanini F. Benatti and M. Piani. *Phys. Rev. Lett.*, 91:070402, 2003.

[71] F. Benatti and R. Floreanini. *Int. J. Quant. Inf.*, 4(3):395, 2006.

[72] S. Oh and J. Kim. *Phys. Rev. A*, 73:062306, 2006.

[73] R.-F. Liu and C.-C. Chen. *Phys. Rev. A*, 74:024102, 2006.

[74] S.-J. Wang J.-H. An and H.-G. Luo. *Physica A*, 382:753, 2007.

[75] S. Natali and Z. Ficek. *Phys. Rev. A*, 75:042307, 2007.

[76] J. Dajka and J. Łuczka. *Phys. Rev. A*, 77:062303, 2008.

[77] Z. Ficek and R. Tanaś. *Phys. Rev. A*, 77:054301, 2008.

[78] S. Shresta C. Anastopoulos and B. L. Hu. *arXiv:quant-ph/0610007v2.*

[79] P. Zanardi and M. Rasetti. *Phys. Rev. Lett.*, 79:3306, 1997.

[80] P. Zanardi. *Phys. Rev. A*, 56:4445, 1997.

[81] R. L. Zaffino N. Lo Gullo S. Maniscalco, F. Francica and F. Plastina. *Phys. Rev. Lett.*, 100:090503, 2008.

[82] G. R. Guthöhrlein *et al. Nature*, 41:449, 2001.

[83] P. Maunz *et al. Nature*, 50:428, 2004.

[84] A. Wallraff *et al. Nature*, 431:162, 2004.

[85] J. I. Park M.A. Sillanpää and R. W. Simmonds. *Nature*, 449:438, 2007.

[86] J. Majer *et al. Nature*, 449:443, 2007.

[87] F. W. Cummings M. Tavis. *Phys. Rev.*, 170:379, 1968.

[88] G. C. Guo S. B. Zheng. *Phys. Rev. Lett.*, 85:2392, 2000.

[89] A. Wallraff S. M. Girvin A. Blais, R.-S. Huang and R. J. Schoelkopf. *Phys. Rev. A*, 69:062320, 2004.

[90] M. Schaefer L. Roa, R. Pozo-González and P. Utreras-SM. *Phys. Rev. A*, 75:062316, 2007.

[91] S. Olivares S. Maniscalco and M. G. A. Paris. *Phys. Rev. A*, 75:062119, 2007.

[92] V. Frerichs and A. Schenzle. *Phys. Rev. A*, 44:1962, 1991.

[93] V.L.S. Schulman. *Phys. Rev. A*, 57:1509, 1998.

[94] J.J. Bollinger W.M. Itano, D.J. Heinzen and D.J. Wineland. *Phys. Rev. A*, 41:2295, 1990.

[95] B. Gutierrez-Medina M.C. Fisher and M.G. Raizen. *Phys. Rev. Lett.*, 87:040402, 2001.

[96] A.G. Kofman and G Kurizki. *Nature (London)*, 405:546, 2000.

[97] A.G. Kofman and G Kurizki. *Phys. Rev A*, 54:3750, 1996.

[98] H. Nakazato P. Facchi and S. Pascazio. *Phys. Rev. Lett.*, 86:2699, 2001.

[99] B. Misra and E.C.G. Sudarshan. *J. Math. Phys.*, 18:756, 1977.

[100] P. Facchi *et al. Phys. Rev. A*, 71:022302, 2005.

[101] Y. Piilo F. Plastina F. Francica, S. Maniscalco and K-A Suominen. *Phys. Rev. A*, 79:032310, 2009.